Paz-Cedeno, FR.; Carceller-Carceller, JM.; Iborra Chornet, S.; Keitel Donato, R.; Ruiz Rodriguez, AF.; Morales, MA.; Solorzano-Chavez, EG.... (2022). Stability of the Cellic CTec2 enzymatic preparation immobilized onto magnetic graphene oxide: Assessment of hydrolysis of pretreated sugarcane bagasse. Industrial Crops and Products. 183:1-14. https://doi.org/10.1016/j.indcrop.2022.114972

Industrial Crops & Products

Stability of the Cellic CTec2 enzymatic preparation immobilized onto magnetic graphene oxide: Assessment of hydrolysis of pretreated sugarcane bagasse

--Manuscript Draft--

Manuscript Number:	INDCRO-D-22-00520R2
Article Type:	Research Paper
Section/Category:	Biorefinery, valorization of byproducts
Keywords:	Sugarcane bagasse; Enzyme immobilization; Enzymatic hydrolysis; Biocatalyst reuse; Second-generation ethanol; Magnetic graphene oxide
Corresponding Author:	Fernando Roberto Paz Cedeno, Ph.D. BRAZIL
First Author:	Fernando Roberto Paz Cedeno, Ph.D.
Order of Authors:	Fernando Roberto Paz Cedeno, Ph.D.
	Jose Miguel Carceller, PhD
	Sara Iborra, PhD
	Ricardo Keitel Donato, PhD
	Anselmo Fortunato Ruiz Rodriguez, PhD
	Marco Antonio Morales, PhD
	Eddyn Gabriel Solorzano Chavez
	Ismael Ulises Miranda Roldan, PhD
	Ariela Veloso de Paula, PhD
	Fernando Masarin, PhD
Abstract:	Sugarcane bagasse (SB) was subjected to enzymatic hydrolysis using an enzyme cocktail immobilized on magnetic graphene oxide particles (GO-MNP). The thermal, storage, pH, and operational stabilities of the immobilized enzymes, including exoglucanase, endoglucanase, β-glucosidase, xylanase, and β-xylosidase, were evaluated. The half-life of the biocatalyst (GO-MNP-Enz) was longer than that of the free enzymes at temperatures above 45 °C, with the exception of endoglucanase. SB was subjected to pretreatments generating sulfite-NaOH pretreated SB (SSB) and chlorite pretreated SB (CSB). The enzymatic hydrolysis of SSB and CSB was evaluated using free enzymes and GO-MNP-Enz. The cellulose and xylan conversion of SSB using free enzymes was higher than using GO-MNP-Enz; however, a similar result was obtained after 72 h. This did not occur in the hydrolysis of CSB, in which at the end of 72 h, conversion using GO-MNP-Enz did not reach the levels obtained with free enzymes. GO-MNP-Enz was successfully reused in several SSB hydrolysis cycles, maintaining an efficiency of approximately 80% and presenting the highest turnover frequency when compared with previous results reported in literature. Finally, these results show that the immobilization of cellulases and xylanases improves their operational stability and the obtained GO-MNP-Enz can be used for various SB hydrolysis cycles

Dear Editor-in-Chief Runcang Sun, Ph.D.

We would like to thank you and the Reviewers for taking the time to review our manuscript. We truly appreciate your comments and suggestions. Requirements and clarifications of the Reviewers has been addressed and incorporated into the paper. Below we send a list of responses to each of the comments.

Best regards,

Dr. Fernando Roberto Paz Cedeno

LIST OF RESPONSES

Editors' and Reviewers' comments:

The authors studied the stability of the Cellic CTec2 enzymatic preparation immobilized onto magnetic graphene oxide: Assessment of hydrolysis of pretreated sugarcane bagasse. The study is interesting, however, there are some concerns like indistinct explain and insufficient discussion be addressed before publishing it.

1. **How to define the activity of 100% in Figure 3? The optimal temperature and pH of free and immobilized endoglucanase were different for endoglucanase, exoglucanase, β-glucosidase, xylanase, and β-xylosidase, how to select them in section 3.5?**

In all cases, 100% relative activity of free or immobilized enzyme is defined as the maximum activity obtained for the specific assay. Optimum temperature and pH assays seek to verify changes in the optimal conditions of the enzyme after immobilization. Alterations were verified in relation to the optimum temperature for endoglucanase and xylanase, in addition to alterations in the optimum pH of endoglucanase. Enzymatic hydrolysis assays cannot always be conducted under optimal conditions for all enzymes involved in the reaction. However, knowing the optimal conditions for each of the enzymes can be useful to benefit the performance of one or the other.

2. **Line 412, the authors just say they are in agreement with the literature, and they should explain why the optimal temperature and pH were altered after immobilization?**

We agree with the reviewer in his comment. We have added text on lines 401-402

3. **The storage stability of free enzyme should be added to compare with the immobilized enzyme.**

We appreciate the reviewer's comment. The stability of the enzyme cocktail was not altered in the 45 days of evaluation. We have added a text on lines 434-435 explaining that the activity of the enzyme cocktail was 100% during the entire period evaluated.

4. **How to define the "relative activity" in Figure 5 and Figure 7?**

In all cases, 100% relative activity of free or immobilized enzyme is defined as the maximum activity obtained for the specific assay. All activities are reported as a percentage of the maximum activity obtained.

5. **The aim of this study was not pretreatment, and the Figure 6 and 8 should be removed to supplement file.**

We appreciate the editor/reviewer's comment. Accordingly, we have placed Figure 8 in the supplemental information document. Figure 6 (now Figure 4) remains in the main document as it shows the half-life of free and immobilized enzymes.

6. **Cellulose/xylan conversion mean glucose/xylose yield?**

They are basically the same. Cellulose and xylan conversion indicates how much cellulose or xylan was converted to glucose or xylose, respectively. Cellulose and xylan conversion were calculated from equations 7 and 8 of the manuscript.

7. **What is the temperature and pH used in Figure 9? Whether they were the same? However, the optimal of temperature and pH for free and immobilized enzymes was different.**

The temperature and pH used in the hydrolysis tests were 45°C and 4.8, respectively, as indicated in item 2.10. Enzymatic hydrolysis assays cannot always be conducted under optimal conditions for all enzymes involved in the reaction. However, knowing the optimal conditions for each of the enzymes can be useful to benefit the performance of one or the other.

8. **There were large gap for free and immobilized enzymes in cellulose/xylan conversion with two times dosage of immobilized enzymes. So the authors should considering the value of immobilized enzymes because of their additional operation and cost.**

We agree with the reviewer on this comment. There is a large difference in the conversion of cellulose and xylan at the beginning of the reaction. However, the results show that after 72 h the cellulose and xylan conversions reached high levels, being approximately 90 and 100% with loads of 10 and 20 $FPU.g^{-1}$, respectively. Immobilized enzymes will undoubtedly have a higher operational cost compared to free enzymes, but that cost could be overcome by reusing the enzymes.

9. **How to get the cellulose conversion of 100% in Figure 10b?**

Figure 10 shows the conversion of cellulose and xylan after enzymatic hydrolysis, using free and immobilized enzymes. In the case of Figure 10b it can be seen that the conversion percentage slightly exceeds 100%. This can be explained by a set of

factors such as standard deviation, inaccurate chemical composition and the presence of sugars in the commercial enzyme cocktail. All of these factors may have contributed to a conversion rate slightly above 100%.

10. The definition of images should be enhanced, and there were too many images, some should remove to supplement file.

We agree with the editor/reviewer on this comment. We have transferred Figures 1, 2 and 8 to the supplemental information document (now Figures S1, S2 and S5). Additionally, we have made available a document with the figures in better resolution.

The manuscript described the stability of the Cellic CTec2 enzymatic preparation immobilized onto magnetic graphene oxide. In previous study, the authors have prepared and characterized Cellic CTec2 covalently immobilized on a graphene oxide-magnetite nanocomposite (GO-MNP). The stability and reusability were already verified by the hydrolysis of a pretreated SB. So, what is the significant progress of this work compared with previous work?

We appreciate the editor/reviewer's comment. In our previous article (10.1016/j.renene.2020.09.059) the preparation of a biocatalyst (GO-MNP-Enz) composed of enzymes from the Cellic CTec2 cocktail immobilized on graphene oxide-magnetite nanocomposite was studied. In that article we focused on evaluating the performance of the immobilization, the reuse of the catalyst with different specific synthetic substrates for each immobilized enzyme and we carried out only one hydrolysis test of pretreated sugarcane bagasse. In this article we have focused on evaluating the half-life time of each enzyme, the storage stability and the alterations that occur when enzymes are immobilized (optimum pH and temperature of each enzyme separately). Additionally, we carry out several hydrolysis tests on bagasse subjected to different pre-treatments and the respective reuse of the biocatalyst.

For CSB hydrolysis, the conversion using GO-MNP-Enz did not reach the levels obtained with free enzymes.

In the hydrolysis of CSB with immobilized enzymes, the conversion levels that were reached with free enzymes were not reached. However, in the SSB hydrolysis, after 72 h of hydrolysis with immobilized enzyme, the conversion of cellulose and xylan was approximately the same as using free enzymes. This shows that the catalyst has the potential to be used in the hydrolysis of lignocellulosic biomass as long as an adequate pretreatment is applied.

What is the different between the substrate of SSB and CSB?

Sulfite-pretreated sugarcane bagasse (SSB) and chlorite-pretreated sugarcane bagasse (CSB) are sugarcane bagasse subjected to different pretreatments. Item 2.7 describes in detail the procedure for each pretreatment.

The content of acetyl in substrate should be determined. As can be seen from FT-IR, the presence of acetyl groups (~1735 cm-1) on the xylan of CSB, which may hinder the accessibility of cellulase and xylanase to substrate.

We agree with the comment of the editor/reviewer. We have added the acetyl content in Table 1

The reason for the different enzymatic digestion for SSB and CSB should be discussed.

We appreciate the editor/reviewer's comment. Lines 589-595 discuss differences in enzymatic hydrolysis.

HIGHLIGHTS

- Half-life of GO-MNP-Enz was longer than free enzymes at operational temperature
- Similar cellulose and xylan conversion was achieved using GO-MNP-Enz and free enzymes
- GO-MNP-Enz was reused in several cycles of SB hydrolysis maintaining 80% of efficiency
- GO-MNP-Enz presented a high turnover frequency in the pretreated SB hydrolysis

Stability of the Cellic CTec2 enzymatic preparation immobilized onto magnetic graphene oxide: Assessment of hydrolysis of pretreated sugarcane bagasse

Fernando Roberto Paz-Cedeno[*a], Jose Miguel Carceller[b], Sara Iborra[b], Ricardo Keitel Donato[c], Anselmo Fortunato Ruiz Rodriguez[d], Marco Antonio Morales[e], Eddyn Gabriel Solorzano-Chavez[a], Ismael Ulises Miranda Roldán[a], Ariela Veloso de Paula[a], and Fernando Masarin[a]

[a]São Paulo State University (UNESP), School of Pharmaceutical Science (FCF), Department of Bioprocess Engineering and Biotechnology. Araraquara-SP, Brazil. 14800-903

[b]Universitat Politècnica de València (UPV), Institute of Chemical Technology (ITQ), Valencia, Spain. 46022

[c]National University of Singapore, Center for advanced 2D materials. Singapore. 117546

[d]Federal University of Acre, Laboratory of Nanobiotechnology. Rio Branco-AC, Brazil. 69920-900

[e]Federal University of Rio Grande do Norte, Department of Theoretical and Experimental Physics. Natal-RN, Brazil. 59078-970.

(*) Corresponding author

Email addresses:

FRPC: fernando.paz@unesp.br
JMC: jocarca8@upvnet.upv.es
SI: siborra@itq.upv.es
RKD: donato@nus.edu.sg
AFRR: anselmo.rodriguez@ufac.br
MAM: morales@fisica.ufrn.br
EGSC: eddyn.solorzano@unesp.br
IUMR: imiranda_3@hotmail.com
AVP: ariela.veloso@unesp.br
FM: fernando.masarin@unesp.br

ABSTRACT

Sugarcane bagasse (SB) was subjected to enzymatic hydrolysis using an enzyme cocktail immobilized on magnetic graphene oxide particles (GO-MNP). The thermal, storage, pH, and operational stabilities of the immobilized enzymes, including exoglucanase, endoglucanase, β-glucosidase, xylanase, and β-xylosidase, were evaluated. The half-life of the biocatalyst (GO-MNP-Enz) was longer than that of the free enzymes at temperatures above 45 °C, with the exception of endoglucanase. SB was subjected to pretreatments generating sulfite-NaOH pretreated SB (SSB) and chlorite pretreated SB (CSB). The enzymatic hydrolysis of SSB and CSB was evaluated using free enzymes and GO-MNP-Enz. The cellulose and xylan conversion of SSB using free enzymes was higher than using GO-MNP-Enz; however, a similar result was obtained after 72 h. This did not occur in the hydrolysis of CSB, in which at the end of 72 h, conversion using GO-MNP-Enz did not reach the levels obtained with free enzymes. GO-MNP-Enz was successfully reused in several SSB hydrolysis cycles, maintaining an efficiency of approximately 80% and presenting the highest turnover frequency when compared with previous results reported in literature. Finally, these results show that the immobilization of cellulases and xylanases improves their operational stability and the obtained GO-MNP-Enz can be used for various SB hydrolysis cycles.

Keywords: Sugarcane bagasse; Enzyme immobilization; Enzymatic hydrolysis; Biocatalyst reuse; Second-generation ethanol; Magnetic graphene oxide.

1. INTRODUCTION

Owing to its abundance and wide availability, lignocellulosic biomass is an alternative to reduce the dependence on petroleum derivatives in the manufacture of fuels and chemical products. Sugarcane bagasse (SB) is the most abundant lignocellulosic biomass in Brazil. In the 2019/2020 season, sugarcane crops had a dry weight of 643 million tons, of which SB represented approximately 14% (CONAB, 2020). SB is an economical and sustainable biomass for obtaining value-added products, such as bioethanol (Alokika et al., 2021; Jugwanth et al., 2020; Sritrakul et al., 2017), biodiesel (Brar et al., 2017), biobutanol (Li et al., 2017; Tsai et al., 2020), biohydrogen (Jiang et al., 2016; Srivastava et al., 2021), xylitol (Morais Junior et al., 2019), citric acid (Kumar et al., 2003), succinic acid (Xu et al., 2021), itaconic acid (Nieder-Heitmann et al., 2018), lactic acid (Nalawade et al., 2020), butyric acid (Wei et al., 2013), gluconic acid (Zhou and Xu, 2019), furfural (Li et al., 2021), oligosaccharides (Barbosa et al., 2020; Zhou and Xu, 2019), and reducing sugars (de Cassia Pereira Scarpa et al., 2019; Paz-Cedeno et al., 2021, 2020) among others.

Enzymatic hydrolysis is an important step in the process of obtaining bioproducts from SB; however, the use of free enzymes can increase the production costs. The immobilization of enzymes onto solid supports and their reuse in several hydrolysis cycles has proven to be a technically feasible strategy to minimize this problem (Gao et al., 2018; Han et al., 2018; Paz-Cedeno et al., 2020).

Additionally, the immobilization of enzymes confers several advantages to the biocatalyst, such as higher thermal or pH stability, and from an industrial point of view, it facilitates the easy separation of the catalyst and bioproducts (Carceller et al., 2019). However, despite the possibility of enzymatic hydrolysis of untreated SB, the application of pretreatments that partially remove lignin from SB reduces recalcitrance

and improves the results of enzymatic hydrolysis (Paz-Cedeno et al., 2021). In fact, lignin limits the hydrolysis of biomass, restricting the access of enzymes to cellulose, thereby acting as a physical barrier (Laureano-Perez et al., 2005). Therefore, the removal of lignin increases the specific area of the biomass, which further enhances the enzyme accessibility.

In a previous study, we prepared and characterized an enzymatic cocktail of cellulases and xylanases covalently immobilized on a graphene oxide-magnetite nanocomposite (GO-MNP) (Paz-Cedeno et al., 2020). Preliminary results of the hydrolysis of a pretreated SB showed that the biocatalyst exhibited excellent stability and reusability, giving a turnover frequency (TOF) that was higher than the one obtained in previous studies. Therefore, in order to optimize the industrial applicability and productivity of the biocatalyst (GO-MNP-Enz), further research is required on the optimization of reaction parameters. Consequently, in this study, the effects of pH and temperature on the activities of endoglucanase, exoglucanase, β-glucosidase, xylanase, and β-xylosidase were investigated along with their thermal, pH, and storage stabilities. Additionally, a comparison study was performed to estimate the influence of two different SB pretreatments in response to enzymatic hydrolysis using free and GO-MNP-Enz forms under the optimal reaction conditions. This study will provide a better understanding of the characteristics of the biocatalyst, which used in its optimal conditions, could contribute to the reduction of costs and improvement of the productivity of the process for obtaining value added chemicals and renewable biofuels.

2. MATERIALS AND METHODS

2.1. Synthesis of GO-MNP and immobilization of Cellic CTec 2

Initially, graphene oxide (GO) was synthesized via an adaptation of Hummers' method (Hummers and Offeman, 1958; Paz-Cedeno et al., 2020). Graphite powder (99.99%, <150 mm; Sigma Aldrich, St. Louis, MO, USA) was mixed with sulfuric acid (H_2SO_4) (95–97%, v/v) and oxidized to graphite oxide using potassium permanganate ($KMnO_4$). Then, a graphite oxide suspension (5 $mg.mL^{-1}$) was sonicated for 2 h to exfoliate GO. For GO magnetization, $FeCl•6H_2O$ and $FeCl_2•4H_2O$ (molar ratio 2:1) were mixed in an acetic acid solution (3%, v/v) under stirring, and GO (5 $mg.mL^{-1}$) was added. The temperature was raised to 80 °C and ammonia (25%, v/v) was added to increase the pH. After 20 min, the reaction was stopped, and with the help of an external magnetic field, the solid was recovered and washed several times with methanol and ultrapure water. The solid was oven-dried at 40 °C and stored. This material was sonicated in an aqueous suspension before further use to form a homogeneous and stable GO-MNP dispersion.

The commercial Cellic CTec 2 enzymatic cocktail (Novozymes, Denmark) was immobilized on the surface of the GO-MNP support, forming GO-MNP-Enz. For this, the functionalization of the support (20 mL of GO-MNP dispersion at 0.5 $mg.mL^{-1}$) with N-hydroxysuccinimide (NHS) (20 mg) and 1-ethyl-3-(-3-dimethylaminopropyl) carbodiimide hydrochloride (EDC) was carried out for 3 h. The functionalized support was washed and resuspended in sodium acetate buffer (pH 4.8). The Cellic CTec 2 enzyme extract was added and the suspension was placed on a roller shaker for 12 h. An external magnet was used to recover GO-MNP-Enz, which was washed and resuspended in the sodium acetate buffer (pH 4.8) (Paz-Cedeno et al., 2020).

2.2. Magnetization and Mössbauer spectroscopy

The magnetic characterization of the GO-MNP samples was performed using a vibrating sample magnetometer (VSM) (model 7400 Lake Shore, Woburn, MA, USA). The isothermal magnetization, M-H curves, were recorded at 300 K with a maximum magnetic field of 15 kOe. The Fe magnetic behavior was studied by ^{57}Fe Mössbauer spectroscopy in the transmission mode at 300 K using a spectrometer (SEE Co., Minneapolis, MN, USA) with a ^{57}Co source with 15 mCi. Isomer shifts were given relative to the isomer shifts of the metallic iron. The spectra were fitted using the Normos90 software.

2.3. Enzyme activity assays and determination of protein content

Cellic CTec2 enzymatic preparation contains several enzymes necessary for the hydrolysis of lignocellulosic biomass, such as endoglucanase, exoglucanase, xylanase, β-glucosidase, and β-xylosidase.

Endoglucanase activity was determined according to the methodology described by Tanaka et al. (1981). Briefly, 0.1 mL volume of diluted Cellic CTec 2 was added to 0.9 mL of 0.44% (w/v) sodium carboxymethylcellulose (CMC) (≥95%; Carbosynth, USA) and kept at 50 °C in a thermal bath for 1 h. Xylanase activity was measured following the methodology described by Bailey et al. (1992). Then, 0.1 mL volume of diluted Cellic CTec 2 was added to 0.9 mL of 1% (w/v) xylan from beechwood (≥90%; Sigma-Aldrich, St. Louis, MO, USA) and kept at 50 °C in a thermal bath for 5 min. Total cellulase activity was determined according to the method described by Ghose (1987) and expressed as filter paper units (FPU). A strip of filter paper (Whatman N°1) was placed in a tube with 1mL of 0.05 M sodium acetate buffer (pH 4.8). Then, Cellic CTec 2 (0.5 mL) was added to the tubes and kept at 50 °C for 1

h. The reactions of endoglucanase, xylanase, and total cellulase were stopped by adding 3,5-dinitrosalicylic acid (DNS) and boiling for 5 min. After cooling, the absorbance was measured at 540 nm using a spectrophotometer.

Exoglucanase, β-glucosidase, and β-xylosidase activities were measured following the methodology described by Tan et al. (1987). Accordingly, 0.8 mL of 0.1% (w/v) 4-nitrophenyl β-D-glucopyranoside (≥98%; Sigma-Aldrich, St. Louis, MO, USA), 4-nitrophenyl β-D-xylopyranoside (≥98%; Sigma-Aldrich, St. Louis, MO, USA), or 4-nitrophenyl β-D-cellobioside (≥98%; Sigma-Aldrich, St. Louis, MO, USA) was added to 0.2 mL of diluted Cellic CTec 2 and kept at 50 °C in a thermal bath for 30 min. The reactions were stopped by adding 2 mL of 10% (w/v) sodium bicarbonate ($NaHCO_3$), and the absorbance was read at 410 nm.

The protein content of Cellic CTec 2 was determined using the method described by Bradford (1976). Accordingly, a volume of properly diluted enzyme preparation was mixed with the Bradford reagent (Sigma-Aldrich, St. Louis, MO, USA), and absorbance was measured using a spectrophotometer at 595 nm. A standard curve was constructed using bovine serum albumin (BSA; Sigma-Aldrich, St. Louis, MO, USA).

According to Sheldon and Van Pelt (2013), the most used parameters to determine the success of enzyme immobilization are immobilization yield, immobilization efficiency, and activity recovery. In this context, we calculated these parameters using the following equations:

$$Yield = \left(\frac{A_i - A_f}{A_i}\right) * 100\% \quad (1)$$

$$Efficiency = \left(\frac{A_b}{A_i - A_f}\right) * 100\% \quad (2)$$

$$Activity\ recovery = \left(\frac{A_b}{A_i}\right) * 100\% \quad (3)$$

where A_i is the total activity of the enzyme cocktail solution before immobilization, A_f is the total activity of the supernatant after immobilization, and A_b is the total activity of GO-MNP-Enz.

2.4. Determination of maximum activity temperature and pH

The assays to determine the maximum activity temperature and pH were conducted as described in Section 2.2. To determine the maximum activity temperature, the tests were carried out at temperatures between and 30–80 °C, at intervals of 10 °C. To determine the maximum activity pH, the tests were performed at pH 3–8 at the previously defined maximum activity temperature. The data were presented in the form of relative activity, considering 100% of the highest activity obtained.

2.5. Thermal and pH stabilities

The thermal stabilities of endoglucanase, exoglucanase, β-glucosidase, xylanase, and β-xylosidase were determined by incubating the enzymes (free and immobilized) at temperatures of 30, 40, 50, and 60 °C for 72 h. The residual activities of the enzymes were measured at different time intervals. The stability in various pH buffers was determined similarly by incubating the enzymes (free or immobilized) at 4 °C in buffers at pH 3–8 and determining the residual activities.

Additionally, the storage stabilities of immobilized endoglucanase, exoglucanase, β-glucosidase, xylanase, and β-xylosidase were determined by incubating GO-MNP-Enz at 4 °C in sodium acetate buffer (pH 4.8, 0.05 M) for 45 d and measuring the residual activities of the enzymes at several intervals of time. The data are presented as relative activity, considering 100% of the activity observed

immediately after immobilization. Additionally, the storage stability of the dry GO-MNP-Enz was evaluated. For this, GO-MNP-Enz was dried under vacuum conditions at a temperature of 40 °C and then resuspended to measure its enzymatic activity.

2.6. Half-life and enzyme deactivation

For thermal deactivation calculations, it is common to use a first-order kinetic model to correlate the enzymatic activity with time at a specific temperature (Melo, 2003). Considering this, Equations 4 and 5 were used to calculate the thermal deactivation kinetic constant (K_d) and half-life time ($t_{1/2}$) of each immobilized enzyme at different temperatures.

$$Ln\left(\frac{A}{A_0}\right) = -K_d t \quad (4)$$

$$t_{\frac{1}{2}} = \frac{ln\left(\frac{1}{2}\right)}{K_d} \quad (5).$$

where A is the final enzymatic activity of the free or immobilized enzyme, A_0 is the initial enzymatic activity, K_d is the thermal deactivation kinetic constant (h^{-1}), and $t_{1/2}$ is the half-life time of the free or immobilized enzyme.

2.7. Pretreatment of SB

SB was separately subjected to two different pretreatments (Paz-Cedeno et al., 2021). For the first pretreatment, 50 g (dry weight) of SB was placed in a 1.5 L reactor (AU/E-20; Regmed, Osasco-SP, Brazil). Then, 250 mL of 1% (w/v) sodium hydroxide (NaOH) solution and 250 mL of 2% (w/v) sodium sulfite (Na_2SO_3) solution were added. The reactor was configured to operate at 140 °C for 30 min with a horizontal rotation of 4 rpm. The obtained material was washed with tap water until the pH was

neutralized and dried in an oven at 40 °C for 24 h. This material was denoted as sulfite-pretreated SB (SSB).

For the second pretreatment, 20 g (dry weight) of SB was placed in a beaker and 640 mL of ultrapure water, 6 g of sodium chlorite, and 2 mL of acetic acid were added. The reaction was maintained at 70 °C for 4 h. At each hour of the reaction, 6 g of sodium chlorite and 2 mL of acetic acid were added. After pretreatment, the mixture was filtered through a porous glass filter # 3 (Schott, Mainz, Germany) and washed with distilled water until the pH was neutral. The treated SB retained in the filters was washed with 200 mL of pure acetone after neutralization (Siqueira et al., 2011). The material was separated and oven-dried for 24 h at 40 °C. This material was named chlorite-pretreated SB (CSB).

The yield of pretreatments was determined by gravimetry (percentage in relation to initial mass and mass after pretreatment, dry weight).

2.8. Chemical composition of untreated and pretreated SB

To determine the chemical composition of SB, SSB, and CSB, the samples were ground using a knife mill and a 20-mesh sieve (0.84 mm screen). Lignin and carbohydrate content were determined by acid hydrolysis (Masarin et al., 2011). For this, SBs were mixed with 72% (w/w) H_2SO_4 for 1 h at 30 °C, then the H_2SO_4 was diluted to a concentration of 4% (w/w), and the reaction was maintained for 1 h at 121 °C. The hydrolysate was filtered through porous glass filters # 3 (Schott, Mainz, Germany) and the material retained on the filter was washed with ultrapure water, dried, weighed, and considered insoluble lignin. An aliquot of the filtrate was used to determine the soluble lignin via spectrophotometry (205 nm). To determine structural carbohydrates content, the filtrate was injected into a high-performance liquid

chromatography (HPLC) system equipped with an HPX87H column (Bio-Rad, Hercules, CA, USA) at 60 °C with 0.005 M H_2SO_4 at a flow rate of 0.6 mL.min^{-1}. Detection was performed using a refractive index detector (model C-R7A; Shimadzu, Kyoto, Japan) at 60 °C (Masarin et al., 2016; Paz-Cedeno et al., 2021). The cellulose and hemicellulose contents in the SB were calculated from glucose, xylose, arabinose, and acetic acid data.

2.9. Structural characterization of untreated and pretreated SB

The SBs were oven-dried, milled, and sieved using a 0.84 mm screen. The samples were subjected to X-ray diffraction (XRD) using a Kristalloflex diffractometer (Siemens, Munich, Germany), running at a power output of 40 kV with a current of 30 mA and Ka Cu radiation (λ = 1.5406 Å) at 25 °C within an angle range of 5–70° 2Θ (Bragg angle) and a scan speed of 2° min^{-1}. The crystallinity index (CrI) was calculated from XRD using the deconvolution method (curve fitting). PeaKFit software v.4.12 was used for peak fitting, assuming Gaussian functions to approximate each peak (Park et al., 2010; Roldán et al., 2017; Terinte et al., 2011). CrI was calculated using Equation 6, as follows:

$$CrI\ (\%) = \left(\frac{A_c}{A_c + A_a}\right) * 100\% \quad (6)$$

where A_c is the area of the crystalline region and A_a is the area of the amorphous regions.

Scanning electron microscopy (SEM) images were obtained using a JSM-7500F field-emission scanning electron microscope (JEOL, Japan). For this purpose, the samples were thoroughly oven-dried for 24 h at 50 °C, homogenized, and placed on a conductive carbon adhesive tape.

The ground and dried samples of SB were used for molecular absorption spectrophotometry in the UV and visible regions using a Varian Cary 5000 UV- Vis-NIR spectrophotometer (Crawley, UK) with a Cary Praying Mantis diffuse reflectance accessory for dried powder samples. The samples were analyzed at wavelengths of 200–700 nm using MgO as the reference substance.

Infrared analysis was performed using attenuated total reflection with a Fourier transform infrared (ATR-FTIR) spectrometer (Platinum-ATR Alpha; Bruker, Billerica, MA, USA) with a single reflection diamond module at 25 °C.

2.10. Enzymatic hydrolysis of pretreated SB and recycling

Pretreated SB was hydrolyzed (CSB and SSB) using both free and immobilized Cellic CTec 2 enzymatic preparation forms. For this purpose, 100 mg (dry weight) of SB (SSB or CSB) was placed in a beaker and 10 mL of acetate buffer (pH 4.8) containing the appropriate amount of GO-MNP-Enz to reach an enzyme load of 10 and 20 FPU per gram of SB (dry weight) was added. The reaction was carried out in a thermal shaker at 45 °C and 150 rpm for 72 h. Aliquots were withdrawn at certain time intervals and injected into an HPLC system using an HPX87H column (Bio-Rad, Hercules, CA, USA) at 60 °C in the isocratic mode using 0.005 M H_2SO_4 at a rate of 0.6 $mL.min^{-1}$. Detection was performed using a refractive index detector (model C-R7A; Shimadzu, Kyoto, Japan) at 60 °C. The cellulose and xylan conversions were determined using Equations 7 and 8, respectively.

$$Cellulose\ conversion\ (\%) = \left(\frac{M_g * 0.90}{F_C * M_B}\right) * 100\% \quad (7)$$

$$Xylan\ conversion\ (\%) = \left(\frac{M_x * 0.88}{F_X * M_B}\right) * 100\% \quad (8)$$

where M_g is the mass of glucose (mg), 0.9 is the conversion factor of glucose to cellulose, F_C is the cellulose fraction in the pretreated SB ($g \cdot g.g^{-1}$), M_B is the mass of

pretreated SB at the start of the reaction (mg), M_x is the mass of xylose (mg), 0.88 is the conversion factor of xylose to xylan, and F_X is the xylan fraction in the pretreated SB ($g \cdot g.g^{-1}$).

The operational stability of GO-MNP-Enz was assessed in several cycles of hydrolysis of pretreated SB (both SSB and CSB). Hydrolysis was conducted under the same conditions as established above, but only for 24 h. Subsequently, the biocatalyst was retained using an external magnet and the supernatant was removed from the reaction. Then, 100 mg of SB and 10 mL of acetate buffer were added again and placed in a shaker at 45 °C and 150 rpm to start the new hydrolysis cycle. A replicate of the experiment (both SSB and CSB) was carried out separately for the recovery of GO-MNP-Enz to perform SEM, as previously described.

2.11. Estimation of kinetic parameters

A model based on saturation kinetics was used to interpret the glucose and xylose concentrations obtained during the enzymatic hydrolysis assays (Paz-Cedeno et al., 2019). For this purpose, Equation 9 was used:

$$C = C_{Max}(1 - e^{-kt}) \quad (9)$$

where C is the sugar concentration ($g.L^{-1}$), C_{Max} is the asymptotic maximum sugar concentration ($g.L^{-1}$), k is the kinetic constant of sugar accumulation (h^{-1}), and t is the hydrolysis time (h).

3. RESULTS

3.1. Immobilization of Cellic CTec 2 on GO-MNP

Following the methodology described above, GO was obtained from graphite and used to form GO-MNP. This nanocomposite was functionalized to serve as an

immobilization support for the enzymes contained in the commercial enzymatic preparation Cellic CTec 2. After immobilization, the GO-MNP-Enz obtained showed activity of exoglucanase, endoglucanase, β-glucosidase, xylanase, and β-xylosidase of 763, 300, 4500, 1034, and 33 $U.g^{-1}$, respectively, while the total cellulase activity was 44 $FPU.g^{-1}$. The immobilization yield was used to describe the percentage of total enzyme activity from the immobilized free enzyme solution (Sheldon and van Pelt, 2013). Most of the enzymes evaluated in this study obtained a high immobilization yield, ranging between 63% and 97%, with the exception of xylanase, which was 27%. The immobilization efficiency is described as the percentage of bound enzyme activity that was verified in GO-MNP-Enz. Most of the time, this value is less than 100%, likely because of mass transfer limitations, tertiary structure modifications, decreased accessibility of active sites, and solubility of the specific substrate for each enzyme assay (Boudrant et al., 2020). In this study, exoglucanase and β-glucosidase showed efficiency values greater than 100% (136% and 113%, respectively), indicating that these enzymes are less sensitive to mass transfer issues, presumably because of the high solubility of the specific substrates. Lastly, the activity recovery compares the activity verified in GO-MNP-Enz to that of the total starting activity of the free enzyme and shows the potential for success of the immobilization process. The values presented in Table S1 were published in a previous article by our research group, with the exception of the values referring to exoglucanase (Paz-Cedeno et al., 2020).

3.2. Magnetic properties and Mössbauer spectroscopy

Figure S1 shows the Mössbauer spectra of GO-MNP and GO-MNP-Enz at room temperature. The spectra were fitted to a six-line spectrum with a distribution of hyperfine magnetic fields (Bhf). Both distributions indicated a high spectral contribution

of Fe ions in a Bhf of 45 T, which is close to the expected values for either magnetite or maghemite nanoparticles (Cornell and Schwertmann, 2006). At low Bhf, the GO-MNP-Enz sample has a higher spectral contribution, indicating the presence of a larger number of smaller nanoparticles, probably because of the wide distribution of particle sizes. Both spectra indicate the presence of Fe oxide nanoparticles with slow relaxing magnetic moments, that is, within the measurement window time of the Mössbauer technique ($\approx 10^{-8}$ s), the nanoparticles were thermally blocked at 300 K.

The room-temperature magnetization measurements are shown in Figure S2. These curves show hysteresis behavior with very small remanence magnetization (Mr = 3.8-3.9 emu.g^{-1}) compared with the saturation magnetization (Ms = 54-64.5 emu.g^{-1}) and low values of the coercivity field (Hc = 35-41 Oe). The low values of Mr/Ms ($\approx$ 0.065) and Hc indicate an ensemble of nanoparticles in the superparamagnetic regime. The Ms values were obtained from the law to the approach to saturation by fitting the magnetization data obtained in a magnetic field (H) above 8 kOe to the equation M=Ms(1-A/H), where A is a constant (Chikazumi, 1997). The differences observed in the Mössbauer and magnetometry studies are ascribed to the different values of the measurement window times of the Mössbauer spectroscopy ($\approx 10^{-8}$ s) and magnetometry ($\approx$ 1–10 s) techniques. That is, at a given temperature, the Fe magnetic moment in a nanoparticle may be frozen in the window time of 10^{-8} s, and it may be fast relaxing in the window time of 1 s. The lower value of Ms, compared with bulk magnetite, is attributed to the mass content of graphene and enzyme. Furthermore, small nanoparticles have a very large surface area per gram of sample and usually present many defects at their surface, which may lead to a decrease in their magnetization. Because the nanoparticles exhibit superparamagnetic behavior at 300 K, in the absence of an external magnetic field, their magnetization appears to be

on average zero, and in the presence of a gradient field, the nanoparticles may be dragged out.

3.3. Optimal temperature, pH, and stability

Cellic CTec 2 enzymes in free and immobilized forms were evaluated to determine the optimal temperature and pH in response to enzyme activity (Figure 1). Endoglucanase and xylanase activities showed differences in relation to the optimal temperature in the free and immobilized forms. For these enzymes, the optimal temperature was 60 °C for the free form, but decreased to 50 °C for the immobilized form. Changes in the temperature and pH of maximum activity are usually attributed to alterations in the structure of the enzymes promoted by the immobilization process. Exoglucanase, β-glucosidase, and β-xylosidase did not show differences between the free and immobilized forms, with an optimal temperature of 60 °C for exoglucanase, 50-60 °C for β-glucosidase, and 50 °C for β-xylosidase. These results are in agreement with the literature, as several studies have shown little or no difference in optimal temperature between immobilized and free cellulases and xylanases (Poorakbar et al., 2018; Sui et al., 2019; Terrasan et al., 2016; Wang et al., 2018).

The optimum pH of all the enzymes was the same in the free and immobilized forms, except for endoglucanase, which showed an optimum pH of 4 in free form and 5 in immobilized form. These results agree with those reported by Wang et al. (2018) using endoglucanase immobilized on magnetic gold mesoporous silica nanoparticles. However, the literature shows different results in this regard. Huang et al. (2020) immobilized endoglucanase in magnetic Fe_2O_3/Fe_3O_4 nanocomposites and reported a decrease in the optimal pH from 5 to 4, compared with the free form, while Sui et al. (2019) immobilized endoglucanase in polyurea microspheres and did not observe an

optimal pH change between free and immobilized enzymes, with an optimal pH of 5. In the case of xylanase, the relative activity at all pH values was similar in the free and immobilized forms, with the exception of pH 3, in which the enzyme in the immobilized form maintains a relative activity close to 100%, while in the free form, relative activity was approximately 35%.

Figure 1. Optimal temperature and pH of free and immobilized endoglucanase **(a-b)**, exoglucanase **(c-d)**, β-glucosidase **(e-f)**, xylanase **(g-h)**, and β-xylosidase **(i-j)**. Non-visible standard deviations indicate that the marker is greater than the deviation itself.

The storage stability of GO-MNP-Enz was also assessed. A suspension of GO-MNP-Enz (1 $mg.mL^{-1}$) was refrigerated (4 °C) and the residual activity was measured. After 45 d, the enzymatic activities remained between 65 and 82% (Figure 2). Additionally, the GO-MNP-Enz activity was evaluated after being subjected to a vacuum drying. The dry GO-MNP-Enz immediately showed a great loss of activity, probably because of the difficulty in forming a dispersion again. In future tests, the storage stability in a more concentrated dispersion will be evaluated to reduce the amount of water in storage. The storage stability of the commercial enzyme cocktail was not altered during the evaluated period.

Figure 2. Storage stabilities of immobilized endoglucanase, exoglucanase, β-glucosidase, xylanase, and β-xylosidase. Non-visible standard deviations indicate that the marker is greater than the deviation itself.

The thermal stability of enzymes is a vital parameter from the point of view of industrial application. In this study, we evaluated the thermal stability of endoglucanase, exoglucanase, β-glucosidase, xylanase, and β-xylosidase in a temperature range of 30–60 °C for 72 h (Figure 3). It was possible to verify that the immobilization of the enzymes in GO-MNP played an important role in the improvement of the thermal stability of the enzymes at temperatures up to 45 °C.

However, this effect was less evident at temperatures above 50 °C, which was reflected in the half-life time (Figure 4). Sui et al. (Sui et al., 2019) evaluated the thermal stability (at 50 °C) of free and immobilized endoglucanase from commercial preparation (cellulase from *Aspergillus niger*, Shanghai Macklin Biochemistry Technology Co. Ltd) on polyurea microspheres and reported that after 3 h, the activity of the free endoglucanase decreased up to 30% of its initial activity, while the immobilized enzyme decreased to approximately 85%. Gouda and Abdel-Naby (2002) evaluated the stability of free and immobilized xylanase (produced by the authors from *Aspergillus tamarii*) on a support denominated Duolite A147; after 3 h of incubation at 40, 50, and 60 °C, the activity of the free xylanase decreased to 50, 30, and 10%, respectively. In the case of immobilized xylanase, a small improvement was observed, with the activity falling to 70, 40, and 15% after 3 h at 40, 50, and 60 °C, respectively.

The half-life of the enzymes in the free and immobilized forms was calculated at temperatures between 30 °C and 60 °C (Figure 3). At a low temperature (30 °C), the free enzyme presented stable activity values; therefore, it was not possible to calculate the half-life time, with the exception of xylanase, which presented a loss of activity at 30 °C and a half-life of 68 h, and in the immobilized form it was 492 h. We verified that at 45 °C, the half-life of the immobilized form was longer than that of the free form; in all cases, with the exception of endoglucanase, where the half-life time in the free form was greater than 200 h. From an industrial point of view, this result is very interesting because a longer half-life time is related to the longer operational stability of GO-MNP-Enz with the associated economic benefits. Additionally, it is possible to verify that the half-life time decreases dramatically at 50 °C compared to 45 °C, indicating that in an enzymatic hydrolysis assay, the enzymes will maintain their activity for a longer time at 45 °C.

Figure 3. Thermal stabilities of free and immobilized endoglucanase, exoglucanase, β-glucosidase, xylanase, and β-xylosidase. Non-visible standard deviations indicate that the marker is greater than the deviation itself.

Figure 4. Half-life time of free and immobilized endoglucanase **(a)**, xylanase **(b)**, exoglucanase **(c)**, β-xylosidase **(d)**, and β-glucosidase **(e)**.

Figure 5. pH stabilities of free and immobilized endoglucanase, exoglucanase, β-glucosidase, xylanase, and β-xylosidase. Non-visible standard deviations indicate that the marker is greater than the deviation itself.

The free and immobilized enzymes were incubated in buffer with a pH between 3 and 8 to evaluate their stability (Figure 5). Free and immobilized exoglucanase maintained relative activity greater than 70% after 72 h, in all cases, with the exception of pH 3 and 4 of the free form, where a significant drop was observed. Free and immobilized endoglucanase maintained a relative activity greater than 80% at all pH values. The immobilized β-glucosidase presented a better stability than the free β-glucosidase at pH values of 5, 6, 7, and 8; however, at pH 3, it lost 60% of its activity. The xylanase and β-xylosidase enzymes showed a relative activity greater than 60% at all pH values after 72 h.

3.4. Chemical composition and structural analysis of pretreated SB

The literature shows that enzymatic hydrolysis of untreated SB is inefficient, and there is a need to subject the biomass to a pretreatment in order to reduce the recalcitrance presented by these materials (Paz-Cedeno et al., 2021). Untreated SB contained 34.6% cellulose, 25.3% hemicellulose, 21.9% lignin, 3.7% ash, and 7.8% extractives, constituting a total of 93.3%. According to the literature (Sluiter et al., 2010), the hemicellulose chains of grasses often contain methyl glucuronic acid, which is added to the oxidation products of sugars (hydroxymethylfurfural, furfural, formic,

and levulinic acid), is part of the indeterminate components that complete the chemical composition of SB (Table 1).

Table 1. Chemical composition of untreated and pretreated sugarcane bagasse (SB).

SB was subjected to two different pretreatments using sulfite-NaOH and sodium chlorite. The visual aspect of SB changed, leaving the pretreated samples clearer than the untreated sample (Figure S3). The SEM images show morphological differences between the untreated and pretreated SB. Figure S4a shows a mostly smooth and uniform structure, characteristic of untreated SB, while Figures S4b and S2c show rough and irregular structures, which are the result of the deconstruction of the cell wall caused by the pretreatments (SSB and CSB, respectively).

After the pretreatments, the percentages of the components of the SB changed, with the main result being the removal of lignin, which decreased to approximately 10% (raw material, Table 1). The data presented in Table 1 show that there was no significant loss of cellulose content after pretreatment. However, there was a significant loss of hemicellulose in the sulfite-NaOH pretreatment (33%), while pretreatment with sodium chlorite did not show significant differences. In relation to lignin, it was verified that the two pretreatments were successful in removing it, as pretreatment with sulfite-NaOH reduced more (71.3%) than pretreatment with chlorite (61.0%). Ashes were incorporated into the pretreated samples, as the mass balance indicates that it was contaminated with inorganics during pretreatment, resulting in a content of 6.1 and 8.5% for SSB and CSB, respectively. Mendes et al. (2011) subjected SB to pretreatment with sulfite-NaOH at 120 °C for 1 h and reported a 53.3% removal of lignin. Applying a pretreatment with sodium chlorite in SB, Siqueira et al. (2013) reported a 70% decrease in lignin content, which is consistent with the results presented in this study.

The ATR-FTIR spectra of SB, SSB, and CSB are shown in Figure S5a. The spectra show characteristic bands of cellulose (bands *g*, *h*, *j,* and *k*), hemicellulose (band *c*), and lignin (bands *a, b, d, e, f, i*, and *l*). A detailed description of the bands is provided in Table S2. In this study, the spectra were compared to confirm their chemical composition. In this sense, it is possible to verify that the characteristic bands of cellulose are present in all the spectra, confirming that the pretreatments did not degrade it. Band *c*, typical of hemicellulose, is present in the SB and CSB spectra; however, this band is not found in the SSB spectrum, confirming the decrease in the hemicellulosic fraction in SSB, as shown in Table 1. Regarding lignin, a decrease in the intensity of the characteristic bands was observed in the spectra of SSB and CSB compared to the spectrum of SB, confirming the decrease of this component in the pretreated SB.

The UV-Vis spectra of the samples are shown in Figure S5b. The bands at 280 and 350 nm correspond to the non-conjugated and conjugated phenolic groups present in biomass containing lignin, respectively (Arun et al., 2020). SB shows a maximum absorption peak at approximately 350 nm, which can be attributed to the coniferyl aldehyde structures, ρ-coumaric and ferulic acids in lignin (Bu et al., 2011; Jääskeläinen et al., 2006). The SSB and CSB spectra show a shift in the region of maximum absorbance from 350 nm to 280–310 nm, compared to SB, indicating that the characteristic components of the 350 nm region (conjugated phenolic groups) were partially removed. The SSB and CSB maximum absorbance region (280–310 nm) are related to lignin rich in guaiacyl-syringyl and hydroxycinnamic acids (Yang et al., 2013). This result indicates a partial decrease in the lignin content, corroborating the results of the chemical composition (Table 1).

552 Figure S5c presents the X-ray diffractogram and crystallinity index (CrI) of SB,
553 SSB, and SCB. The SB presented a CrI of 45.5%, which is consistent with that
554 reported in the literature (Paz-Cedeno et al., 2021; Roldán et al., 2017). After the
555 pretreatments, an increase in CrI was verified, with an SSB of 61.1% and CSB of
556 54.6%. Lignin and hemicellulose have amorphous structures, and their removal favors
557 an increase in the CrI of the biomass under study. These results agree with those
558 reported in Table 1, confirming that lignin and hemicellulose were partially removed in
559 SSB. In contrast, in CSB, the hemicellulose content remains the same despite the
560 removal of lignin, which is reflected in a lower CrI in CSB than in SSB.
561

562 ### 3.5. Enzymatic hydrolysis of pretreated SB

563 Untreated SB can be directly subjected to enzymatic hydrolysis. However, as
564 has been widely demonstrated in the literature (Mesquita et al., 2016; Paz-Cedeno et
565 al., 2021; Tavares et al., 2018; Terán Hilares et al., 2018), this biomass exhibits a high
566 recalcitrance against enzymatic hydrolysis, which generally leads to cellulose and
567 xylan conversion values of approximately 20% or less. Consequently, SSB and CSB
568 were subjected to pretreatment to improve the enzymatic hydrolysis performance. The
569 profile of enzymatic hydrolysis of SSB and CSB using free and immobilized Cellic
570 CTec 2 is presented in Figure 6.

571 **Figure 6.** Hydrolysis of sulfite-NaOH (SSB) **(a-b)** and chlorite (CSB) **(c-d)** pretreated
572 SB using free and immobilized enzymes. Non-visible standard deviations indicate that
573 the marker is greater than the deviation itself.
574

575 The conversion of cellulose and xylan into glucose and xylose was faster in
576 tests performed with the enzyme in its free form compared to the immobilized form.
577 This is probably due to the mass-transfer limitation problems faced by immobilized
578 enzymes (Boudrant et al., 2020). After 72 h of hydrolysis, the cellulose conversion

reached 100% in both SSB and CSB. In the case of xylan conversion, we verified that after 72 h of hydrolysis of SSB, it reached 100% conversion, but in the CSB, it reached approximately 80%.

The results of hydrolysis of SSB using immobilized enzymes show that, despite the fact that in the first hours, the conversion is lower compared to hydrolysis with free enzymes form, after 72 h, the cellulose and xylan conversions reached high levels, being approximately 90 and 100% with loads of 10 and 20 $FPU.g^{-1}$, respectively. Meanwhile, the results of the hydrolysis of CSB show that although an increase in the load of immobilized enzymes (from 10 to 20 $FPU.g^{-1}$) increases the cellulose conversion (from 60 to 87%) and xylan conversion (from 44 to 67%), it is not enough to reach the levels of conversion achieved by the free enzyme form. These differences may be due to the fact that the SSB promotes the sulfonation of lignin, which increases the swelling of the fibers and, in this way, increases the exposure of cellulose and hemicellulose to the active sites of the enzymes (Mendes et al., 2011; Paz-Cedeno et al., 2021). Additionally, the sulfonated lignin is more hydrophilic and presents less unproductive adsorption of the enzymes, which makes the reuse of GO-MNP-Enz more efficient (Mendes et al., 2013). Siqueira et al. (2011) subjected SB to pretreatment with chlorite and verified the response to enzymatic hydrolysis with free enzyme form. The data presented by the authors are lower than those found in this work, reaching a cellulose conversion of 60% into glucose and 55% conversion of xylan into xylose after 72 h of hydrolysis.

The kinetic parameters calculated from the experimental data, using a previously reported mathematical model (Oliveira et al., 2018; Paz-Cedeno et al., 2019; Solorzano-Chavez et al., 2019), helped us to understand the differences in the kinetics of free and immobilized enzyme forms (Table 2). In all cases, the maximum

rate of product formation was higher in the free form than in the immobilized form. However, it was verified that in the case of SSB hydrolysis, there was no significant difference in the maximum rate of glucose formation between hydrolysis with an enzyme load of 10 and 20 FPU.g^{-1}, but there was a difference in the maximum rate of xylose formation, with 20 FPU.g^{-1} higher. On the other hand, there was a significant difference between the hydrolysis of CSB that used 10 and 20 FPU.g^{-1}, as the hydrolysis with 20 FPU.g^{-1} had a higher rate of both glucose and xylose formation.

Table 2. Kinetic parameters of enzymatic hydrolysis of pretreated SB using free and immobilized enzymes.

3.6. Operational stability of GO-MNP-Enz

The main objective of enzyme immobilization was the reuse of GO-MNP-Enz in several cycles of hydrolysis. For this reason, enzymatic hydrolysis tests of SSB and CSB were performed using immobilized enzymes, and after the hydrolysis cycle was finished, the GO-MNP-Enz was recovered with the aid of an external magnet and reused in a new hydrolysis cycle (Figure 7).

Figure 7. Recycling hydrolysis of sulfite-NaOH (SSB) **(a-b)** and chlorite (CSB) **(c-d)** pretreated SB.

The hydrolysis of SSB with immobilized enzymes (enzyme load 10 FPU.g^{-1}) resulted in cellulose conversion into glucose of 47% in the first cycle and remained at a similar level until the fourth cycle when it reached 36% (Figure 7a). Xylan conversion into xylose in the same test was 45% in the first cycle and 39% in the last cycle. Although these values are not high, a very low loss of GO-MNP-Enz efficiency was confirmed between hydrolysis cycles, maintaining an efficiency of 76% and 86% in the cellulose and xylan conversions, respectively, compared to the first cycle. Carrying out the same hydrolysis test but with a higher enzymatic load (20 FPU.g-1), it was verified

631 that the cellulose conversion was 74% in the first cycle and remained at a similar level
632 until the fourth cycle, reaching 62% (Figure 7b). In the same test, the xylan conversion
633 in the first cycle was 74% and 63% in the fourth cycle. This indicates that the efficiency
634 of GO-MNP-Enz was approximately 84% after four cycles of hydrolysis compared to
635 the first cycle. From these SSB hydrolysis tests, we can show that the cellulose and
636 xylan conversions in each hydrolysis cycle increase with the increase in enzymatic
637 load; however, the catalyst efficiency reached similar levels in the tests with 10 and 20
638 $FPU.g^{-1}$.

639 CSB hydrolysis showed inferior performance compared to SSB hydrolysis.
640 Using 10 $FPU.g^{-1}$, the cellulose conversion in the first cycle reached 28% and 9% in
641 the last cycle. The xylan conversion in the first cycle was 23%, and in the fourth cycle
642 it was 5% (Figure 7c). This indicates that the efficiency of GO-MNP-Enz decreased by
643 68% for cellulose conversion and 79% for xylan conversion. The increase in the
644 enzymatic load for 20 $FPU.g^{-1}$ led to an increase in the cellulose and xylan
645 conversions, reaching 54% and 36% in the first cycle, respectively. However, in the
646 fourth cycle, the cellulose conversion barely reached 13%, and xylan conversion was
647 11% (Figure 7d). This indicates that there was a loss of catalyst efficiency of 75% in
648 the case of cellulose conversion and 69% in xylan conversion, compared to the first
649 cycle.

650 These differences in bioconversion of SSB and CSB may be due to the fact that
651 pretreatment with sulfite-NaOH reduces hydrophobic interactions between lignin and
652 the enzyme, achieving less unproductive adsorption and additionally causing a
653 swelling between the fibers that facilitates the access of the GO-MNP-Enz and
654 therefore increases the conversion during the hydrolysis (Mendes et al., 2011).
655 Moreover, the higher cellulose and xylan conversions facilitated the separation of the

GO-MNP-Enz at the time of finishing one hydrolysis cycle and starting the next, since there is less insoluble matter that can adhere to the GO-MNP-Enz.

Finally, the GO-MNP-Enz performance under optimal reaction conditions was compared with previously reported results. Table 3 presents the glucose production values and TOF (h^{-1}) obtained in the hydrolysis of lignocellulosic biomass using immobilized biocatalysts. The GO-MNP-Enz used in this work showed superior performance in terms of TOF compared to those previously reported in the literature, showing the high potential of our GO-MNP-Enz for the industrial production of sugars from SB biomass. In a previous article (Paz-Cedeno et al., 2020), we reported the hydrolysis of SSB using GO-MNP-Enz and obtained a TOF of 0.0006 for glucose production. This value was much lower than that obtained now, probably because the hydrolysis conditions were not optimized. Previously, we worked at a temperature of 30 °C and an enzymatic load of 660 $FPU.g^{-1}$. The evaluation of half-life time, thermal stability, and optimal temperature in this work allowed us to adjust the conditions so that GO-MNP-Enz can work more efficiently. Table 3 presents the glucose production values and TOF obtained in the hydrolysis of lignocellulosic biomass using immobilized biocatalysts.

Table 3. Data on glucose production during the enzymatic hydrolysis of different lignocellulosic biomasses.

4. CONCLUSION

The enzymes contained in the commercial Cellic CTec 2 enzymatic preparation immobilized in GO-MNP showed similar behavior in a wide range of pH and temperature conditions compared to the free form. GO-MNP-Enz was stable during cold storage for 45 d. The half-life time at the operational temperature (45 °C) was higher in GO-MNP-Enz than the free form, with the exception of endoglucanase. This

683 indicates that immobilization favors the operational stability of the enzymes evaluated.
684 Regarding the hydrolysis of pretreated SB, we confirmed that the hydrolysis of SSB
685 was better than that of CSB. This had repercussions in the reuse tests of GO-MNP-
686 Enz, in which it was found that after several cycles of hydrolysis of SSB, the efficiency
687 of GO-MNP-Enz remained at levels between 76% and 86%, while in the hydrolysis of
688 CSB, the efficiency of the catalyst after four cycles of hydrolysis was between 25%
689 and 32%.

690 Finally, the immobilization of enzymes in GO-MNP showed an improvement in
691 the operational stabilities of the evaluated enzymes, maintaining high efficiency after
692 several cycles of hydrolysis and achieving higher productivity than previously reported
693 biocatalysts. Therefore, the use of GO-MNP-Enz can be considered as a technically
694 viable strategy for the hydrolysis of pretreated SB, which could contribute to improving
695 the efficiency of bioprocesses, for example, the production of cellulosic generation
696 ethanol, a renewable and environmentally friendly biofuel.

697

698 ## 5. DECLARATIONS SECTION

699 **List of abbreviations**

700 (ATR-FTIR) Attenuated total reflection-Fourier Transform Infrared; (CMC) Sodium
701 carboxymethylcellulose; (CrI) Crystallinity index; (CSB) Chlorite pretreated SB; (EDC)
702 1-ethyl-3-(3-dimethylaminopropyl) carbodiimide; (EDX) Energy-dispersive X-ray;
703 (FPU) Filter paper units; (GO) Graphene oxide; (GO-MNP) Graphene oxide-magnetite
704 nanocomposite; (GO-MNP-Enz) Biocatalyst; (NHS) *N*-hydroxy-succinimide; (SEM)
705 Scanning electron microscopy; (SB) Sugarcane bagasse untreated; (SSB) Sulfite-
706 NaOH pretreated SB; (TOF) turnover frequency; (TON) turnover number; (XRD) X-ray
707 diffractogram.

Ethical Approval and Consent to participate

Not applicable.

Consent for publication

All authors read and approved the final manuscript.

Availability of supporting data

We are providing a document with supplementary information.

Conflicts of interest

There are no conflicts to declare.

Funding

This work was supported by the São Paulo State Research Support Foundation [grant numbers 2018/06241-3]; the Coordination of Improvement of Higher Education Personnel (CAPES) [grant number 001]; Severo Ochoa Program [grant number SEV-2016-0683]; the Spanish Ministry of Science, Innovation and Universities (MCIU) and Spanish State Research Agency (AEI) [grant number PGC2018-097277-B-100].

CRediT authorship contribution statement

Fernando Roberto Paz Cedeno: Conceptualization, Investigation, Methodology, Writing - original draft, Writing - review & editing. **Jose Miguel Carceller:** Methodology, Writing - review & editing. **Sara Iborra:** Supervision, Funding acquisition, Resources, Writing - review & editing. **Ricardo Keitel Donato:**

Supervision, Writing - review & editing. **Anselmo Fortunato Ruiz Rodriguez**: Methodology, Writing - review & editing. **Marco Antonio Morales:** Methodology, Writing - review & editing. **Eddyn Gabriel Solorzano-Chavez:** Methodology, Writing - review & editing. **Ismael Ulises Miranda Roldán:** Methodology, Writing - review & editing. **Ariela Veloso de Paula:** Writing - review & editing. **Fernando Masarin:** Conceptualization, Supervision, Funding acquisition, Resources, Writing - review & editing.

Acknowledgements

FAPESP, contract number 2018/06241-3 funding this paper. Coordination of Improvement of Higher Education Personnel (CAPES) financed the doctoral scholarship of Fernando Roberto Paz-Cedeno in Brazil and in the Universitat Politècnica de València (UPV), Institute of Chemical Technology (ITQ), Valencia, Spain. Authors acknowledge financial support from PGC2018-097277-B-100 (MCIU/AEI/FEDER,UE) project and Program Severo Ochoa (SEV-2016-0683).

6. REFERENCES

Alokika, Anu, Kumar, A., Kumar, V., Singh, B., 2021. Cellulosic and hemicellulosic fractions of sugarcane bagasse: Potential, challenges and future perspective. Int. J. Biol. Macromol. 169, 564–582. https://doi.org/https://doi.org/10.1016/j.ijbiomac.2020.12.175

Arun, V., Perumal, E.M., Prakash, K.A., Rajesh, M., Tamilarasan, K., 2020. Sequential fractionation and characterization of lignin and cellulose fiber from waste rice bran. J. Environ. Chem. Eng. 8, 104124.

https://doi.org/https://doi.org/10.1016/j.jece.2020.104124

Bailey, M.J., Biely, P., Poutanen, K., 1992. Interlaboratory testing of methods for assay of xylanase activity. J. Biotechnol. 23, 257–270. https://doi.org/10.1016/0168-1656(92)90074-J

Barbosa, F.C., Kendrick, E., Brenelli, L.B., Arruda, H.S., Pastore, G.M., Rabelo, S.C., Damasio, A., Franco, T.T., Leak, D., Goldbeck, R., 2020. Optimization of cello-oligosaccharides production by enzymatic hydrolysis of hydrothermally pretreated sugarcane straw using cellulolytic and oxidative enzymes. Biomass and Bioenergy 141, 105697. https://doi.org/https://doi.org/10.1016/j.biombioe.2020.105697

Boudrant, J., Woodley, J.M., Fernandez-Lafuente, R., 2020. Parameters necessary to define an immobilized enzyme preparation. Process Biochem. 90, 66–80. https://doi.org/10.1016/j.procbio.2019.11.026

Bradford, M.M., 1976. A Rapid and Sensitive Method for the Quantitation Microgram Quantities of Protein Utilizing the Principle of Protein-Dye Binding. Anal. Biochem. 254, 248–254. https://doi.org/10.1016/0003-2697(76)90527-3

Brar, K.K., Sarma, A.K., Aslam, M., Polikarpov, I., Chadha, B.S., 2017. Potential of oleaginous yeast Trichosporon sp., for conversion of sugarcane bagasse hydrolysate into biodiesel. Bioresour. Technol. 242, 161–168. https://doi.org/https://doi.org/10.1016/j.biortech.2017.03.155

Bu, L., Tang, Y., Gao, Y., Jian, H., Jiang, J., 2011. Comparative characterization of milled wood lignin from furfural residues and corncob. Chem. Eng. J. 175, 176–184. https://doi.org/https://doi.org/10.1016/j.cej.2011.09.091

Carceller, J.M., Martínez Galán, J.P., Monti, R., Bassan, J.C., Filice, M., Iborra, S., Yu, J., Corma, A., 2019. Selective synthesis of citrus flavonoids prunin and naringenin

using heterogeneized biocatalyst on graphene oxide. Green Chem. 21, 839–849. https://doi.org/10.1039/c8gc03661f

Chikazumi, S., 1997. Physics of Ferromagnetism. Oxford Science Publications.

CONAB, 2020. Acompanhamento da Safra Brasileira de Cana-de-açucar Safra 2019/20. Brasilia. https://doi.org/2318-7921

Cornell, R.M., Schwertmann, U., 2006. The Iron Oxides: Structure, Properties, Reactions, Occurrences and Uses, 2nd ed. Wiley.

de Cassia Pereira Scarpa, J., Paganini Marques, N., Alves Monteiro, D., Martins, G.M., de Paula, A.V., Boscolo, M., da Silva, R., Gomes, E., Alonso Bocchini, D., 2019. Saccharification of pretreated sugarcane bagasse using enzymes solution from Pycnoporus sanguineus MCA 16 and cellulosic ethanol production. Ind. Crops Prod. 141, 111795. https://doi.org/https://doi.org/10.1016/j.indcrop.2019.111795

Gao, J., Lu, C.-L., Wang, Y., Wang, S.-S., Shen, J.-J., Zhang, J.-X., Zhang, Y.-W., 2018. Rapid immobilization of cellulase onto graphene oxide with a hydrophobic spacer. Catalysts 8, 1–12. https://doi.org/10.3390/catal8050180

Ghose, T.K., 1987. Measurement of cellulase activities. Pure Appl. Chem. 59, 257–268. https://doi.org/10.1351/pac198759020257

Gouda, M.K., Abdel-Naby, M.A., 2002. Catalytic properties of the immobilized Aspergillus tamarii xylanase. Microbiol. Res. 157, 275–281. https://doi.org/https://doi.org/10.1078/0944-5013-00165

Han, J., Wang, Li, Wang, Y., Dong, J., Tang, X., Ni, L., Wang, Lei, 2018. Preparation and characterization of Fe3O4-NH2@4-arm-PEG-NH2, a novel magnetic four-arm polymer-nanoparticle composite for cellulase immobilization. Biochem. Eng. J. 130, 90–98. https://doi.org/10.1016/j.bej.2017.11.008

Huang, W., Pan, S., Li, Y., Yu, L., Liu, R., 2020. Immobilization and characterization of cellulase on hydroxy and aldehyde functionalized magnetic Fe2O3/Fe3O4 nanocomposites prepared via a novel rapid combustion process. Int. J. Biol. Macromol. 162, 845–852. https://doi.org/https://doi.org/10.1016/j.ijbiomac.2020.06.209

Hummers, W.S., Offeman, R.E., 1958. Preparation of Graphitic Oxide. J. Am. Chem. Soc. 80, 1339–1339. https://doi.org/10.1021/ja01539a017

Jääskeläinen, A.-S., Saariaho, A.-M., Vyörykkä, J., Vuorinen, T., Matousek, P., Parker, A.W., 2006. Application of UV-Vis and resonance Raman spectroscopy to study bleaching and photoyellowing of thermomechanical pulps 60, 231–238. https://doi.org/doi:10.1515/HF.2006.038

Jiang, D., Fang, Z., Chin, S.X., Tian, X.F., Su, T.C., 2016. Biohydrogen Production from Hydrolysates of Selected Tropical Biomass Wastes with Clostridium Butyricum. Sci. Rep. 6, 1–11. https://doi.org/10.1038/srep27205

Jugwanth, Y., Sewsynker-Sukai, Y., Gueguim Kana, E.B., 2020. Valorization of sugarcane bagasse for bioethanol production through simultaneous saccharification and fermentation: Optimization and kinetic studies. Fuel 262, 116552. https://doi.org/https://doi.org/10.1016/j.fuel.2019.116552

Kumar, D., Jain, V.K., Shanker, G., Srivastava, A., 2003. Citric acid production by solid state fermentation using sugarcane bagasse. Process Biochem. 38, 1731–1738. https://doi.org/https://doi.org/10.1016/S0032-9592(02)00252-2

Laureano-Perez, L., Teymouri, F., Alizadeh, H., Dale, B.E., 2005. Understanding factors that limit enzymatic hydrolysis of biomass. Appl. Biochem. Biotechnol. 124, 1081–1099. https://doi.org/10.1385/ABAB:124:1-3:1081

Li, H., Xiong, L., Chen, Xuefang, Wang, C., Qi, G., Huang, C., Luo, M., Chen, Xinde,

2017. Enhanced enzymatic hydrolysis and acetone-butanol-ethanol fermentation of sugarcane bagasse by combined diluted acid with oxidate ammonolysis pretreatment. Bioresour. Technol. 228, 257–263. https://doi.org/https://doi.org/10.1016/j.biortech.2016.12.119

Li, Q., Ma, C.-L., Zhang, P.-Q., Li, Y.-Y., Zhu, X., He, Y.-C., 2021. Effective conversion of sugarcane bagasse to furfural by coconut shell activated carbon-based solid acid for enhancing whole-cell biosynthesis of furfurylamine. Ind. Crops Prod. 160, 113169. https://doi.org/https://doi.org/10.1016/j.indcrop.2020.113169

Masarin, F., Cedeno, F.R.P., Chavez, E.G.S., de Oliveira, L.E., Gelli, V.C., Monti, R., 2016. Chemical analysis and biorefinery of red algae Kappaphycus alvarezii for efficient production of glucose from residue of carrageenan extraction process. Biotechnol. Biofuels 9, 122. https://doi.org/10.1186/s13068-016-0535-9

Masarin, F., Gurpilhares, D.B., Baffa, D.C., Barbosa, M.H., Carvalho, W., Ferraz, A., Milagres, A.M., 2011. Chemical composition and enzymatic digestibility of sugarcane clones selected for varied lignin content. Biotechnol. Biofuels 4, 55. https://doi.org/10.1186/1754-6834-4-55

Melo, E.P., 2003. Estabilidade de proteínas, in: Cabral, J.M.S., Aires-barros, M.R., Gama, M. (Eds.), Engenharia Enzimática. Lidel, Lisbon, pp. 67–120.

Mendes, F.M., Laurito, D.F., Bazzeggio, M., Ferraz, A., Milagres, A.M.F., 2013. Enzymatic digestion of alkaline-sulfite pretreated sugar cane bagasse and its correlation with the chemical and structural changes occurring during the pretreatment step. Biotechnol. Prog. 29, 890–895. https://doi.org/10.1002/btpr.1746

Mendes, F.M., Siqueira, G., Carvalho, W., Ferraz, A., Milagres, A.M.F., 2011. Enzymatic hydrolysis of chemithermomechanically pretreated sugarcane bagasse

858 and samples with reduced initial lignin content. Biotechnol. Prog. 27, 395–401.
859 https://doi.org/10.1002/btpr.553
860 Mesquita, J.F., Ferraz, A., Aguiar, A., 2016. Alkaline-sulfite pretreatment and use of
861 surfactants during enzymatic hydrolysis to enhance ethanol production from
862 sugarcane bagasse. Bioprocess Biosyst. Eng. 39, 441–448.
863 https://doi.org/10.1007/s00449-015-1527-z
864 Morais Junior, W.G., Pacheco, T.F., Trichez, D., Almeida, J.R.M., Gonçalves, S.B.,
865 2019. Xylitol production on sugarcane biomass hydrolysate by newly identified
866 Candida tropicalis JA2 strain. Yeast 36, 349–361.
867 https://doi.org/https://doi.org/10.1002/yea.3394
868 Nalawade, K., Baral, P., Patil, Snehal, Pundir, A., Kurmi, A.K., Konde, K., Patil,
869 Sanjay, Agrawal, D., 2020. Evaluation of alternative strategies for generating
870 fermentable sugars from high-solids alkali pretreated sugarcane bagasse and
871 successive valorization to L (+) lactic acid. Renew. Energy 157, 708–717.
872 https://doi.org/https://doi.org/10.1016/j.renene.2020.05.089
873 Nieder-Heitmann, M., Haigh, K.F., Görgens, J.F., 2018. Process design and economic
874 analysis of a biorefinery co-producing itaconic acid and electricity from sugarcane
875 bagasse and trash lignocelluloses. Bioresour. Technol. 262, 159–168.
876 https://doi.org/https://doi.org/10.1016/j.biortech.2018.04.075
877 Oliveira, S.C., Paz-Cedeno, F.R., Masarin, F., 2018. Mathematical modeling of
878 glucose accumulation during enzymatic hydrolysis of carrageenan waste, in: Silva
879 Santos, A. (Ed.), Avanços Científicos e Tecnológicos Em Bioprocessos. Atena
880 Editora, pp. 97–103. https://doi.org/10.22533/at.ed.475180110
881 Park, S., Baker, J.O., Himmel, M.E., Parilla, P.A., Johnson, D.K., 2010. Cellulose
882 crystallinity index: measurement techniques and their impact on interpreting

883 cellulase performance. Biotechnol. Biofuels 3, 10. https://doi.org/10.1186/1754-
884 6834-3-10
885 Paz-Cedeno, F.R., Carceller, J.M., Iborra, S., Donato, R.K., Godoy, A.P., De Paula,
886 A.V., Monti, R., Corma, A., Masarin, F., 2020. Magnetic graphene oxide as a
887 platform for the immobilization of cellulases and xylanases: ultrastructural
888 characterization and assessment of lignocellulosic biomass hydrolysis. Renew.
889 Energy. https://doi.org/10.1016/j.renene.2020.09.059
890 Paz-Cedeno, F.R., Henares, L.R., Solorzano-Chavez, E.G., Scontri, M., Picheli, F.P.,
891 Miranda Roldán, I.U., Monti, R., Conceição de Oliveira, S., Masarin, F., 2021.
892 Evaluation of the effects of different chemical pretreatments in sugarcane
893 bagasse on the response of enzymatic hydrolysis in batch systems subject to high
894 mass loads. Renew. Energy 165. https://doi.org/10.1016/j.renene.2020.10.092
895 Paz-Cedeno, F.R., Solórzano-Chávez, E.G., de Oliveira, L.E., Gelli, V.C., Monti, R., de
896 Oliveira, S.C., Masarin, F., 2019. Sequential Enzymatic and Mild-Acid Hydrolysis
897 of By-Product of Carrageenan Process from Kappaphycus alvarezii. BioEnergy
898 Res. 12, 419–432. https://doi.org/10.1007/s12155-019-09968-7
899 Poorakbar, E., Shafiee, A., Saboury, A.A., Rad, B.L., Khoshnevisan, K., Ma'mani, L.,
900 Derakhshankhah, H., Ganjali, M.R., Hosseini, M., 2018. Synthesis of magnetic
901 gold mesoporous silica nanoparticles core shell for cellulase enzyme
902 immobilization: Improvement of enzymatic activity and thermal stability. Process
903 Biochem. 71, 92–100. https://doi.org/10.1016/j.procbio.2018.05.012
904 Roldán, I.U.M., Mitsuhara, A.T., Munhoz Desajacomo, J.P., de Oliveira, L.E., Gelli,
905 V.C., Monti, R., Silva do Sacramento, L.V., Masarin, F., 2017. Chemical,
906 structural, and ultrastructural analysis of waste from the carrageenan and sugar-
907 bioethanol processes for future bioenergy generation. Biomass and Bioenergy

908 107, 233–243. https://doi.org/10.1016/j.biombioe.2017.10.008
909 Sánchez-Ramírez, J., Martínez-Hernández, J.L., Segura-Ceniceros, P., López, G.,
910 Saade, H., Medina-Morales, M.A., Ramos-González, R., Aguilar, C.N., Ilyina, A.,
911 2017. Cellulases immobilization on chitosan-coated magnetic nanoparticles:
912 application for Agave Atrovirens lignocellulosic biomass hydrolysis. Bioprocess
913 Biosyst. Eng. 40, 9–22. https://doi.org/10.1007/s00449-016-1670-1
914 Sheldon, R.A., van Pelt, S., 2013. Enzyme immobilisation in biocatalysis: Why, what
915 and how. Chem. Soc. Rev. 42, 6223–6235. https://doi.org/10.1039/c3cs60075k
916 Siqueira, G., Milagres, A.M.F., Carvalho, W., Koch, G., Ferraz, A., 2011.
917 Topochemical distribution of lignin and hydroxycinnamic acids in sugar-cane cell
918 walls and its correlation with the enzymatic hydrolysis of polysaccharides.
919 Biotechnol. Biofuels 4, 7. https://doi.org/10.1186/1754-6834-4-7
920 Siqueira, G., Várnai, A., Ferraz, A., Milagres, A.M.F., 2013. Enhancement of cellulose
921 hydrolysis in sugarcane bagasse by the selective removal of lignin with sodium
922 chlorite. Appl. Energy 102, 399–402.
923 https://doi.org/10.1016/j.apenergy.2012.07.029
924 Sluiter, J.B., Ruiz, R.O., Scarlata, C.J., Sluiter, A.D., Templeton, D.W., 2010.
925 Compositional analysis of lignocellulosic feedstocks. 1. Review and description of
926 methods. J. Agric. Food Chem. 58, 9043–9053. https://doi.org/10.1021/jf1008023
927 Solorzano-Chavez, E.G., Paz-Cedeno, F.R., Ezequiel de Oliveira, L., Gelli, V.C.,
928 Monti, R., Conceição de Oliveira, S., Masarin, F., 2019. Evaluation of the
929 Kappaphycus alvarezii growth under different environmental conditions and
930 efficiency of the enzymatic hydrolysis of the residue generated in the carrageenan
931 processing. Biomass and Bioenergy 127.
932 https://doi.org/10.1016/j.biombioe.2019.105254

933 Sritrakul, N., Nitisinprasert, S., Keawsompong, S., 2017. Evaluation of dilute acid
934 pretreatment for bioethanol fermentation from sugarcane bagasse pith. Agric. Nat.
935 Resour. 51, 512–519. https://doi.org/https://doi.org/10.1016/j.anres.2017.12.006
936 Srivastava, N., Alhazmi, A., Mohammad, A., Haque, S., Srivastava, M., Pal, D.B.,
937 Singh, R., Mishra, P.K., Vo, D.V.N., Yoon, T., Gupta, V.K., 2021. Biohydrogen
938 production via integrated sequential fermentation using magnetite nanoparticles
939 treated crude enzyme to hydrolyze sugarcane bagasse. Int. J. Hydrogen Energy.
940 https://doi.org/https://doi.org/10.1016/j.ijhydene.2021.08.198
941 Sui, Y., Cui, Y., Xia, G., Peng, X., Yuan, G., Sun, G., 2019. A facile route to
942 preparation of immobilized cellulase on polyurea microspheres for improving
943 catalytic activity and stability. Process Biochem. 87, 73–82.
944 https://doi.org/https://doi.org/10.1016/j.procbio.2019.09.002
945 Tan, L.U.L., Mayers, P., Saddler, J.N., 1987. Purification and characterization of a
946 thermostable xylanase from a thermophilic fungus Thermoascus aurantiacus.
947 Can. J. Microbiol. 689–691. https://doi.org/10.1139/m87-120
948 Tanaka, M., Taniguchi, M., Matsuno, R., Kamikubo, T., 1981. Purification and
949 Properties of Cellulases from Eupencillium javanicum : Studies on the Re-
950 utilization of Cellulosic Resources(VII). J. Ferment. Technol. 59, 177–183.
951 Tavares, J., Łukasik, R.M., De Paiva, T., Da Silva, F., 2018. Hydrothermal alkaline
952 sulfite pretreatment in the delivery of fermentable sugars from sugarcane
953 bagasse. New J. Chem. 42, 4474–4484. https://doi.org/10.1039/c7nj04975g
954 Terán Hilares, R., Ramos, L., da Silva, S.S., Dragone, G., Mussatto, S.I., Santos, J.C.
955 dos, 2018. Hydrodynamic cavitation as a strategy to enhance the efficiency of
956 lignocellulosic biomass pretreatment. Crit. Rev. Biotechnol. 38, 483–493.
957 https://doi.org/10.1080/07388551.2017.1369932

Terinte, N., Ibbett, R., Schuster, K., 2011. Overview on native cellulose and microcrystalline cellulose I structure studied by X-ray diffraction (WAXD): Comparison between measurement techniques. Lenzinger Berichte 89.

Terrasan, C.R.F., Aragon, C.C., Masui, D.C., Pessela, B.C., Fernandez-Lorente, G., Carmona, E.C., Guisan, J.M., 2016. β-xylosidase from Selenomonas ruminantium: Immobilization, stabilization, and application for xylooligosaccharide hydrolysis. Biocatal. Biotransformation 34, 161–171. https://doi.org/10.1080/10242422.2016.1247817

Tsai, T.-Y., Lo, Y.-C., Dong, C.-D., Nagarajan, D., Chang, J.-S., Lee, D.-J., 2020. Biobutanol production from lignocellulosic biomass using immobilized Clostridium acetobutylicum. Appl. Energy 277, 115531. https://doi.org/https://doi.org/10.1016/j.apenergy.2020.115531

Wang, Y., Chen, D., Wang, G., Zhao, C., Ma, Y., Yang, W., 2018. Immobilization of cellulase on styrene/maleic anhydride copolymer nanoparticles with improved stability against pH changes. Chem. Eng. J. 336, 152–159. https://doi.org/https://doi.org/10.1016/j.cej.2017.11.030

Wei, D., Liu, X., Yang, S.-T., 2013. Butyric acid production from sugarcane bagasse hydrolysate by Clostridium tyrobutyricum immobilized in a fibrous-bed bioreactor. Bioresour. Technol. 129, 553–560. https://doi.org/https://doi.org/10.1016/j.biortech.2012.11.065

Xu, C., Alam, M.A., Wang, Z., Peng, Y., Xie, C., Gong, W., Yang, Q., Huang, S., Zhuang, W., Xu, J., 2021. Co-fermentation of succinic acid and ethanol from sugarcane bagasse based on full hexose and pentose utilization and carbon dioxide reduction. Bioresour. Technol. 339, 125578. https://doi.org/https://doi.org/10.1016/j.biortech.2021.125578

983 Xu, J., Huo, S., Yuan, Z., Zhang, Y., Xu, H., Guo, Y., Liang, C., Zhuang, X., 2011.
984 Characterization of direct cellulase immobilization with superparamagnetic
985 nanoparticles. Biocatal. Biotransformation 29, 71–76.
986 https://doi.org/10.3109/10242422.2011.566326
987 Yang, D., Zhong, L.X., Yuan, T.Q., Peng, X.W., Sun, R.C., 2013. Studies on the
988 structural characterization of lignin, hemicelluloses and cellulose fractionated by
989 ionic liquid followed by alkaline extraction from bamboo. Ind. Crops Prod. 43,
990 141–149. https://doi.org/10.1016/j.indcrop.2012.07.024
991 Zhou, X., Xu, Y., 2019. Integrative process for sugarcane bagasse biorefinery to co-
992 produce xylooligosaccharides and gluconic acid. Bioresour. Technol. 282, 81–87.
993 https://doi.org/https://doi.org/10.1016/j.biortech.2019.02.129
994

Table 1. Chemical composition of untreated and pretreated sugarcane bagasse (SB).

Biomass	Yield (g/100g of SB)	SB components (g/100g of material) Cellulose (%)	Hemicellulose (%)	Acetyl group (%)	Lignin (%)	Ashes (%)
Untreated	-	34.6 ± 2.5	25.3 ± 1.8	2.6 ± 0.2	21.9 ± 0.6	3.7 ± 0.7
SSB	64.2	48.4 ± 2.9	23.0 ± 2.0	n.d.	9.8 ± 1.0	9.5 ± 0.9
CSB	76.7	42.0 ± 0.6	25.1 ± 0.4	3.1 ± 0.2	10.8 ± 0.8	12.2 ± 2.0
		% of components loss (biomass components as g/100g of untreated SB)				
		Cellulose (%)	Hemicellulose (%)		Lignin (%)	Ashes (%)
Untreated	-	34.6[a]	25.3[a]	2.6	21.9[a]	3.4
SSB	64.2	31.1[a]	16.9[b]	n.d.	6.3[c]	6.1
CSB	76.7	32.2[a]	24.4[a]	2.4	8.2[b]	8.5

**Values that do not share a letter are significantly different according to Tukey test (Minitab 19). Extractives in the untreated sample: 7.8 % (grams per 100 grams of SB,* dry *weight).*
SSB: Sulfite-NaOH pretreated SB. CSB: Chlorite pretreated SB. n.d.: not detected

Table 2. Kinetic parameters of enzymatic hydrolysis of pretreated SB using free and immobilized enzymes.

Biomass	Bioproduct	GO-MNP-Enz	k (h^{-1})	C_{Max} ($g.L^{-1}$)	*Maximum rate of product formation ($g.L^{-1}.h^{-1}$)	R^2
SSB	Glucose	Free (10 FPU.g^{-1})	0.242 ± 0.016	5.238 ± 0.212	1.269 ± 0.084[a]	0.907
		Immobilized (10 FPU.g^{-1})	0.025 ± 0.007	5.826 ± 1.502	0.137 ± 0.004[b]	0.975
		Immobilized (20 FPU.g^{-1})	0.030 ± 0.008	6.765 ± 1.517	0.196 ± 0.015[b]	0.961
	Xylose	Free (10 FPU.g^{-1})	0.072 ± 0.002	2.890 ± 0.087	0.209 ± 0.008[a]	0.973
		Immobilized (10 FPU.g^{-1})	0.045 ± 0.011	2.393 ± 0.463	0.105 ± 0.008[b]	0.986
		Immobilized (20 FPU.g^{-1})	0.050 ± 0.010	2.939 ± 0.446	0.143 ± 0.013[c]	0.962
CSB	Glucose	Free (10 FPU.g^{-1})	0.160 ± 0.010	4.482 ± 0.043	0.715 ± 0.040[a]	0.939
		Immobilized (10 FPU.g^{-1})	0.033 ± 0.005	3.047 ± 0.193	0.099 ± 0.009[b]	0.982
		Immobilized (20 FPU.g^{-1})	0.042 ± 0.009	4.276 ± 0.423	0.177 ± 0.018[c]	0.984
	Xylose	Free (10 FPU.g^{-1})	0.085 ± 0.012	2.203 ± 0.054	0.187 ± 0.024[a]	0.953
		Immobilized (10 FPU.g^{-1})	0.034 ± 0.016	1.447 ± 0.370	0.045 ± 0.013[b]	0.988
		Immobilized (20 FPU.g^{-1})	0.049 ± 0.010	1.931 ± 0.204	0.094 ± 0.009[c]	0.987

** The values with the same superscripts do not differ among themselves (significance level of 0.05; Tukey test, Minitab 19). SSB: Sulfite-NaOH pretreated SB. CSB: Chlorite pretreated SB.*

Table 3. Data on glucose production during the enzymatic hydrolysis of different lignocellulosic biomasses.

Biocatalyst	Biomass	Number of cycles	Time per cycle (h)	Mass of biocatalyst in the reaction (mg)	Glucose total production[a]	TOF[b]	Ref.
GO-MNP-Enz	SSB	4	24	22.7	91.3	0.0419	This work
GO-MNP-Enz	SSB	4	24	45.4	145.9	0.0335	This work
GO-MNP-Enz	CSB	4	24	22.7	29.5	0.0136	This work
GO-MNP-Enz	CSB	4	24	45.4	49.8	0.0114	This work
GO-MNP-Enz	SSB	10	24	150.0	21.0	0.0006	(Paz-Cedeno et al., 2020)
Cel-Ch-MNP	Agave fiber	5	20	122.5	76.3	0.0006	(Sánchez-Ramírez et al., 2017)
CBNP	Bagasse	6	72	2027.0	247.5	0.0003	(Xu et al., 2011)
CBNP	Corn Stalk	6	72	2027.0	371.3	0.0004	(Xu et al., 2011)

[a]mg of glucose after all hydrolysis cycles (mg);
[b]mg of glucose per mg of biocatalyst per hour (h^{-1}).
GO-MNP-Enz: Cellic CTec2 enzyme cocktail immobilized on magnetic graphene-oxide particles.
Cel-Ch-MNP: Cellulase immobilized on chitosan-coated magnetic nanoparticles.
CBNP: Cellulase immobilized on magnetic particles.

Figure

Click here to access/download;Figure;Figures.docx

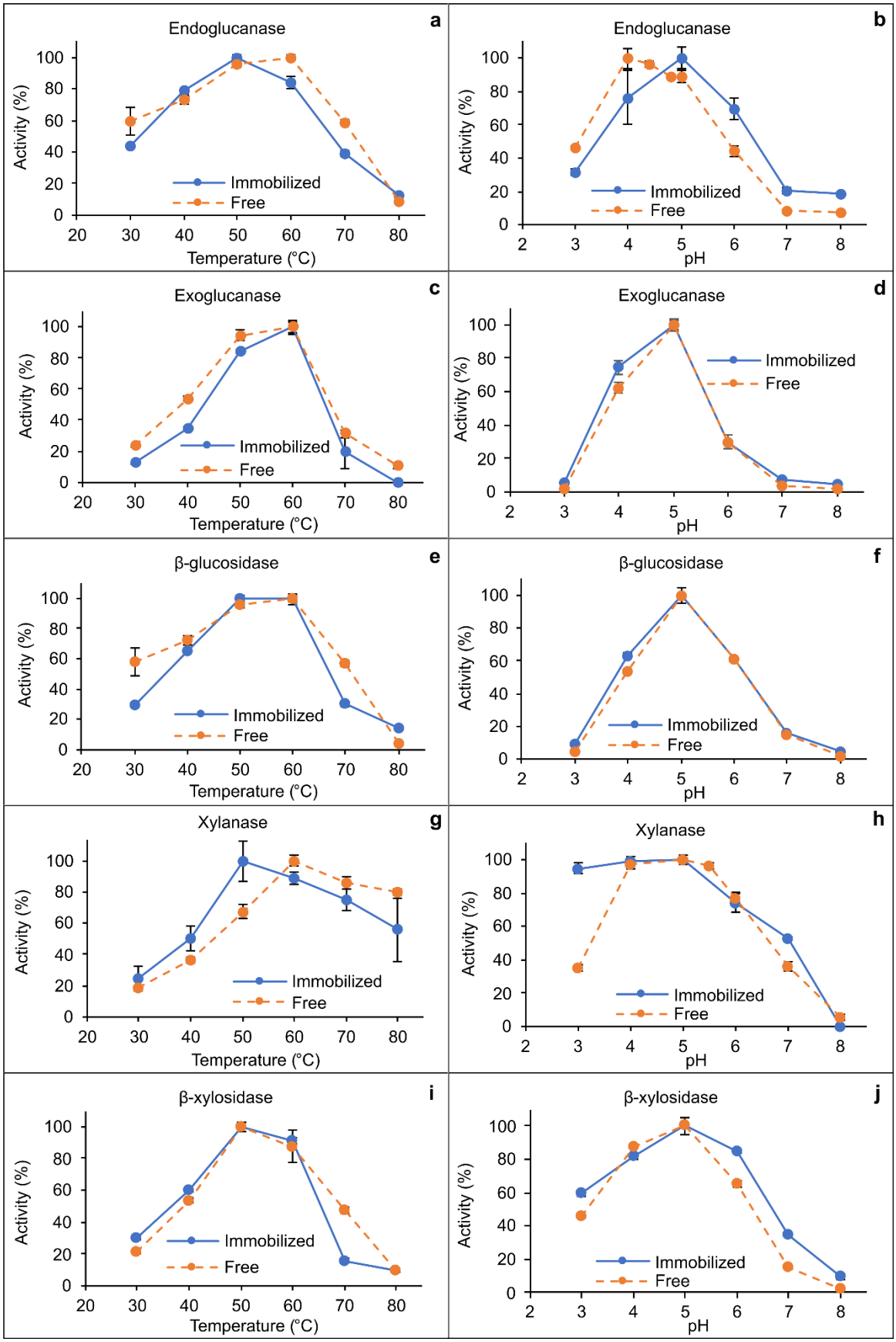

Figure 1. Optimal temperature and pH of free and immobilized endoglucanase **(a-b)**, exoglucanase **(c-d)**, β-glucosidase **(e-f)**, xylanase **(g-h)**, and β-xylosidase **(i-j)**. Non-visible standard deviations indicate that the marker is greater than the deviation itself.

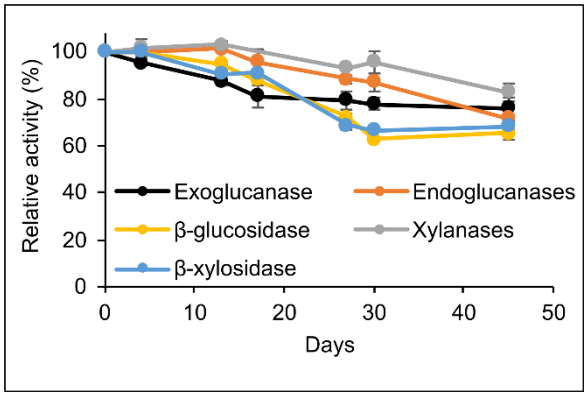

Figure 2. Storage stabilities of immobilized endoglucanase, exoglucanase, β-glucosidase, xylanase, and β-xylosidase. Non-visible standard deviations indicate that the marker is greater than the deviation itself.

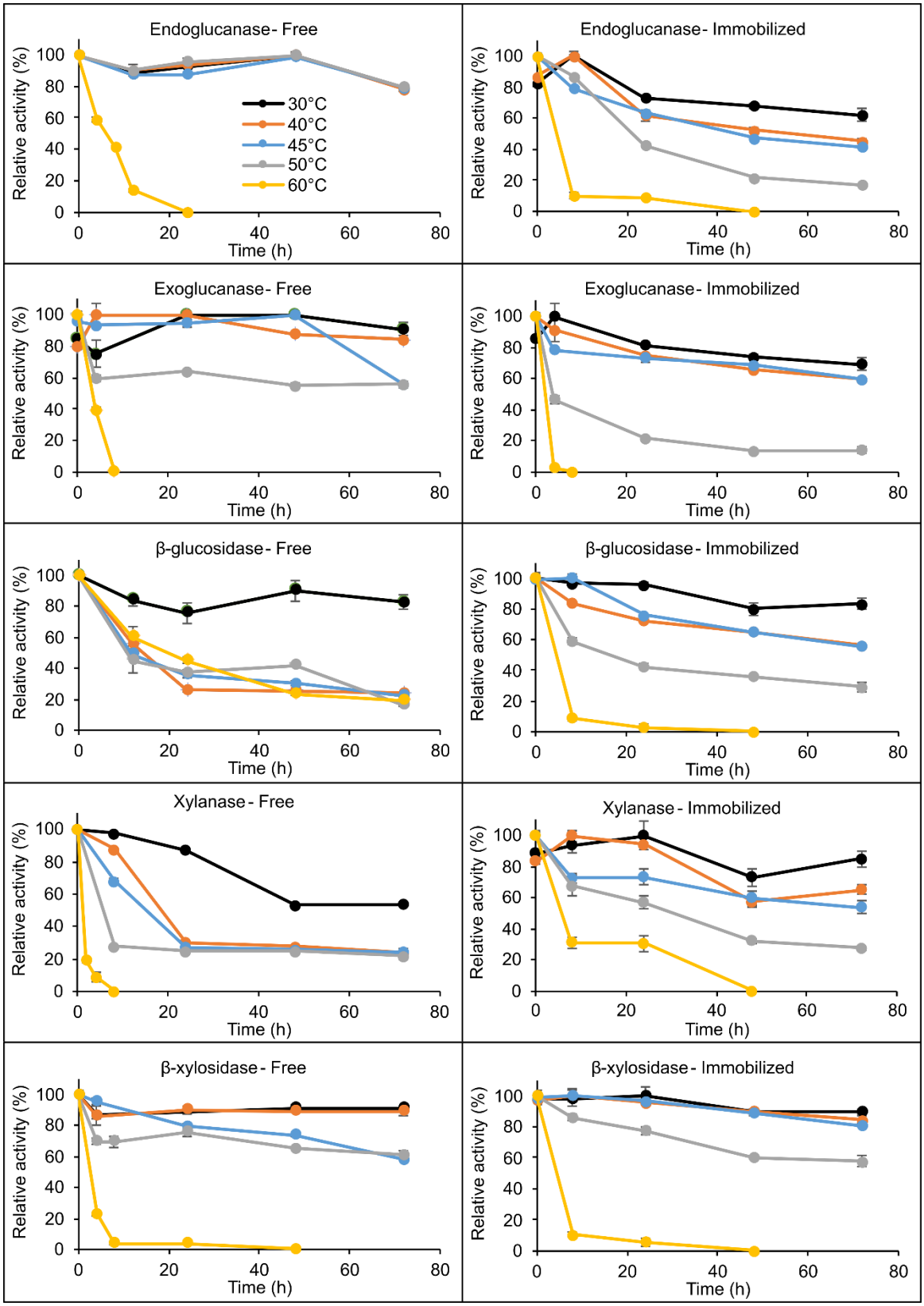

Figure 3. Thermal stabilities of free and immobilized endoglucanase, exoglucanase, β-glucosidase, xylanase, and β-xylosidase. Non-visible standard deviations indicate that the marker is greater than the deviation itself.

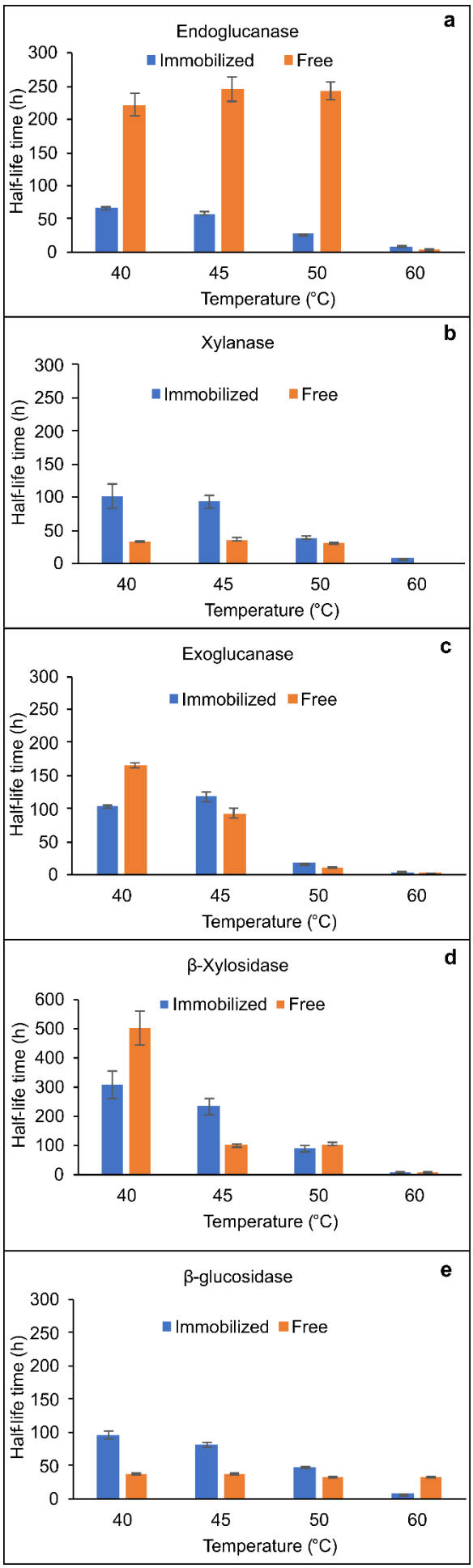

Figure 4. Half-life time of free and immobilized endoglucanase **(a)**, xylanase **(b)**, exoglucanase **(c)**, β-xylosidase **(d)**, and β-glucosidase **(e)**.

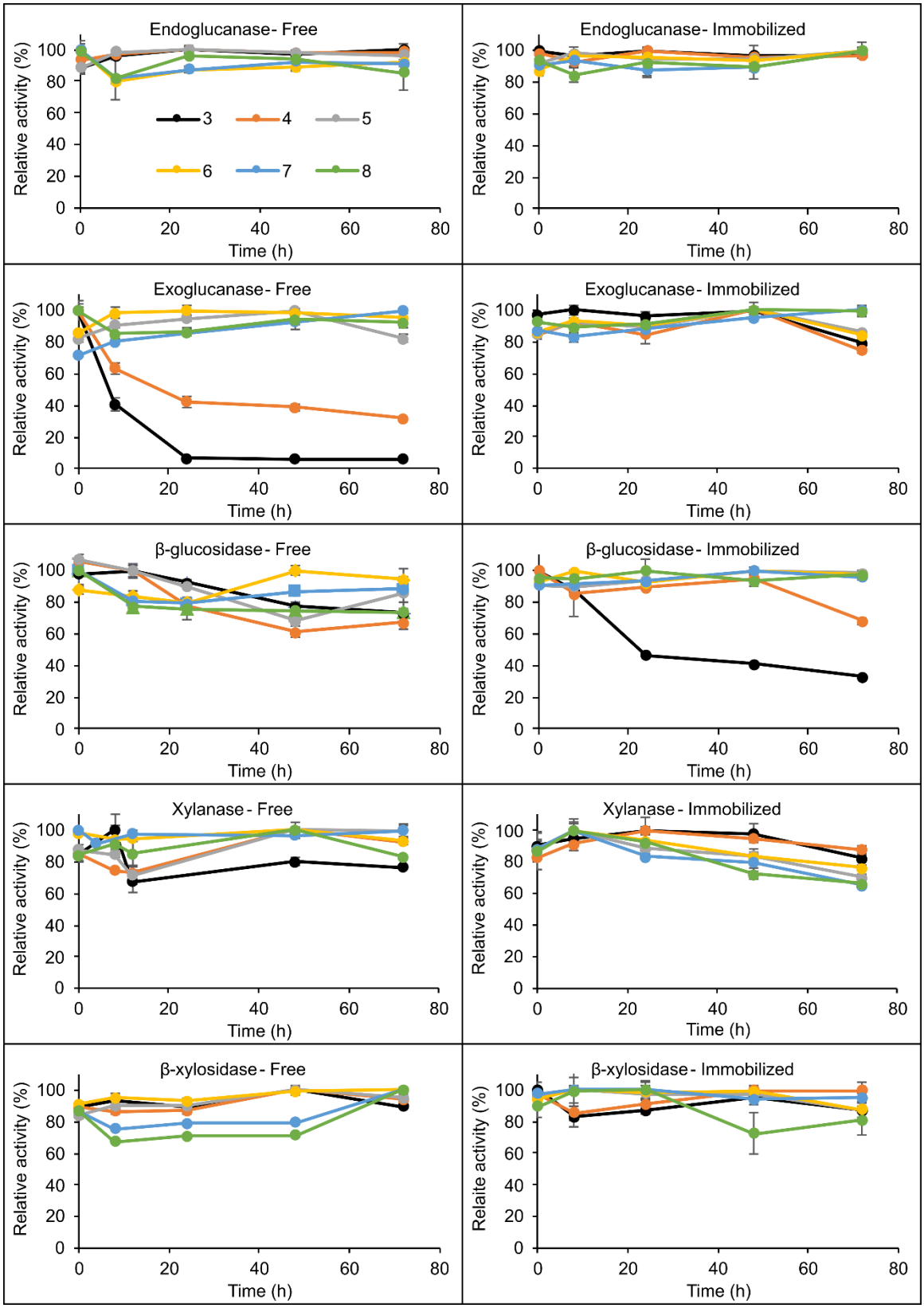

Figure 5. pH stabilities of free and immobilized endoglucanase, exoglucanase, β-glucosidase, xylanase, and β-xylosidase. Non-visible standard deviations indicate that the marker is greater than the deviation itself.

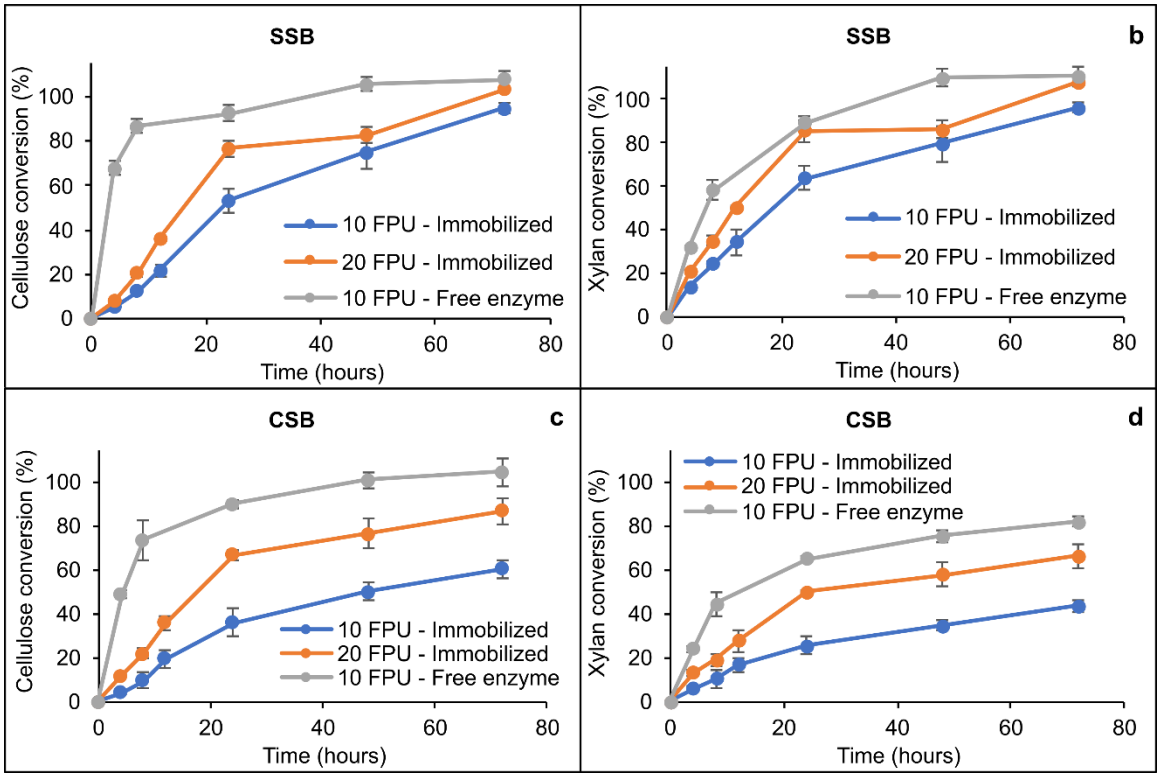

Figure 6. Hydrolysis of sulfite-NaOH (SSB) **(a-b)** and chlorite (CSB) **(c-d)** pretreated SB using free and immobilized enzymes. Non-visible standard deviations indicate that the marker is greater than the deviation itself.

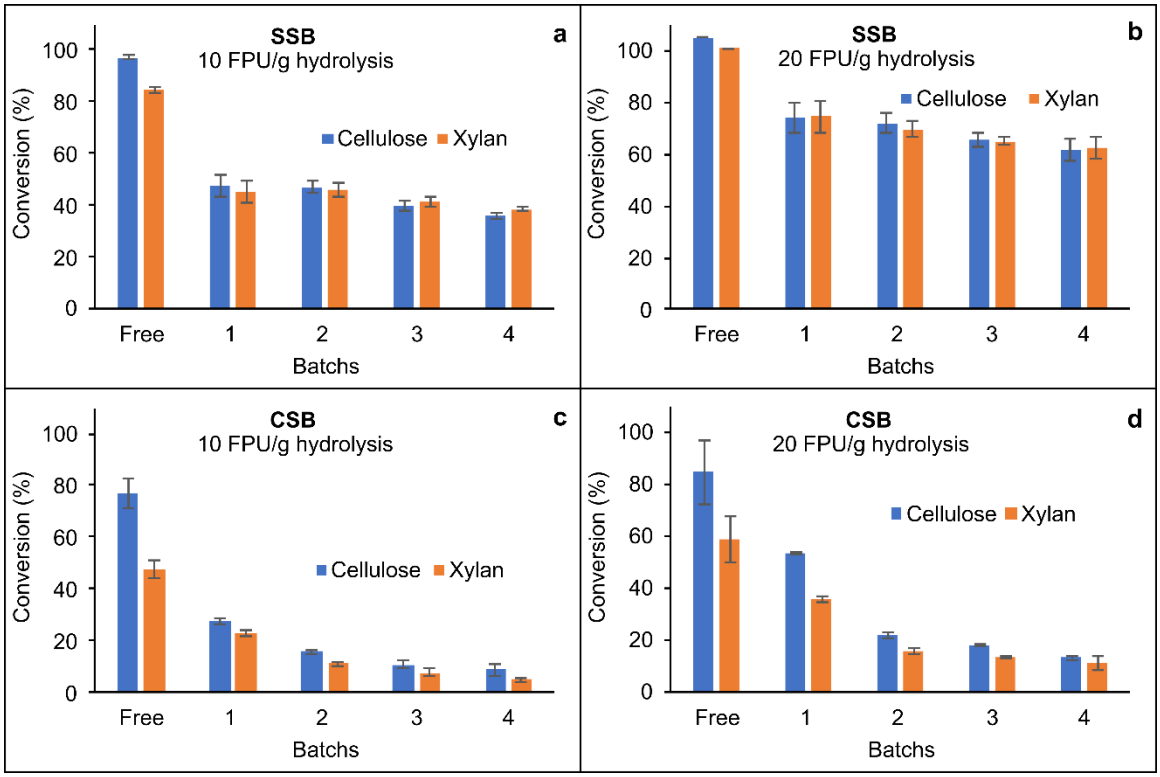

Figure 7. Recycling hydrolysis of sulfite-NaOH (SSB) **(a-b)** and chlorite (CSB) **(c-d)** pretreated SB.

CRediT authorship contribution statement

Fernando Roberto Paz Cedeno: Conceptualization, Investigation, Methodology, Writing - original draft, Writing - review & editing. **Jose Miguel Carceller:** Methodology, Writing - review & editing. **Sara Iborra:** Supervision, Funding acquisition, Resources, Writing - review & editing. **Ricardo Keitel Donato:** Supervision, Writing - review & editing. **Anselmo Fortunato Ruiz Rodriguez**: Methodology, Writing - review & editing. **Marco Antonio Morales:** Methodology, Writing - review & editing. **Eddyn Gabriel Solorzano-Chavez:** Methodology, Writing - review & editing. **Ismael Ulises Miranda Roldán:** Methodology, Writing - review & editing. **Ariela Veloso de Paula:** Writing - review & editing. **Fernando Masarin:** Conceptualization, Supervision, Funding acquisition, Resources, Writing - review & editing.

Declaration of interests

☒The authors declare that they have no known competing financial interests or personal relationships that could have appeared to influence the work reported in this paper.

☐The authors declare the following financial interests/personal relationships which may be considered as potential competing interests: